

The EUMETSAT
 Network of
 Satellite
 Application
 Facilities



Scientific and Validation Report for the Cloud Product Processors of the NWC/PPS

NWC/CDOP2/PPS/SMHI/SCI/VR/Cloud, Issue 1, Rev. 0

15 September 2014

Applicable to SAFNWC/PPS version 2014


Applicable to the following PGE:s:

PGE	Acronym	Product ID	Product name	Version number
PGE01	CM	NWC-62	Cloud Mask	4.0
PGE02	CT	NWC-65	Cloud Type	2.0
PGE03	CTTH	NWC-68	Cloud Top Temperature and Height	4.0
PGE04	PC	NWC-073	Precipitating Clouds	1.6
PGE05	CPP	NWC-71	Cloud Physical Properties	1.1

Prepared by Swedish Meteorological and Hydrological Institute (SMHI)

REPORT SIGNATURE TABLE

Function	Name	Signature	Date
Prepared by	SMHI		15 September 2014
Reviewed by	SAFNWC Project Team EUMETSAT		9 September 2014
Authorised by	Anke Thoss, SMHI <i>SAFNWC PPS Manager</i>		15 September 2014

	Scientific and Validation Report for the Cloud Product Processors of the NWC/PPS	Code: NWC/CDOP2/PPS/SMHI/SCI/VR/Cloud Issue: 1.0 Date: 15 September 2014 File: NWC-CDOP2-PPS-SMHI-SCI-VR-Cloud_v1_0 Page: 3/67
--	--	--

DOCUMENT CHANGE RECORD

Version	Date	Pages	Changes
0.1d	22 January 2014	47	Preliminary version for SAFNWC/PPS v2014
1.0d	27 June 2014	68	First original version for PPS v2014. Updated to be valid for v2014 validation. Implemented action from PCR-v2014: - LSc1,2: (formal issues) - LSc11: added LWP comparison land/sea, using MODIS LWP.
1.0	15 September 2014	67	Implemented RIS from DRR-v2014: -LSc-01, LSc-02, LSc-03, LSc-06

Table of Contents

1	INTRODUCTION	8
1.1	PURPOSE.....	8
1.2	SCOPE.....	8
1.3	DEFINITIONS AND ACRONYMS	8
1.4	REFERENCES.....	9
1.4.1	<i>Applicable documents</i>	9
1.4.2	<i>Reference documents</i>	10
1.5	DOCUMENT OVERVIEW	10
2	DEFINITION OF VERIFICATION MEASURES USED	11
3	DATA USED	13
3.1	THE VIIRS INSTRUMENT ONBOARD SUOMI NPP AND ITS DATA.....	13
3.2	NWP DATA.....	13
3.3	THE SYNOP DATA	13
3.4	THE CALIPSO DATABASE.....	16
3.5	THE AMSR-E DATA SET	22
3.6	THE MODIS LWP DATA SET.....	22
4	RESULTS AND DISCUSSION	24
4.1	CLOUD MASK	24
4.1.1	<i>Synop validation</i>	24
4.1.2	<i>Caliop validation</i>	28
4.2	CLOUD TYPE.....	31
4.3	CLOUD TOP HEIGHT.....	34
4.3.1.1	Study of surface emissivity as input	42
4.4	CLOUD PHYSICAL PROPERTIES	43
4.4.1	<i>CPP cloud phase (cph)</i>	43
4.4.1.1	Study of cloud phase and illumination	46
4.4.1.2	CPH Performance in total	48
4.4.2	<i>CPP liquid water path (lwp)</i>	51
4.4.2.1	LWP validation within the EARS domain	51
4.4.2.2	Study of performance under different illumination conditions.....	56
4.4.2.3	Global validation of LWP	57
4.4.2.4	LWP comparison land/sea.....	60
4.5	PRECIPITATING CLOUDS.....	63
5	SUMMARY AND CONCLUSIONS	64
6	REFERENCES	66
	ANNEX A. LIST OF TBC, TBD, OPEN POINTS AND COMMENTS.....	67

List of Tables and Figures

TABLE 1: LIST OF APPLICABLE DOCUMENTS	10
TABLE 2: LIST OF REFERENCED DOCUMENTS	10
TABLE 3 VALIDATION SCORES FOR 99 GAC ORBITS AGAINST GLOBAL SYNOP REPORTS	24
TABLE 4: VALIDATION SCORES FOR 99 GAC ORBITS AGAINST ONLY THE SYNOP REPORTS WITHIN THE NORTHERN EUROPEAN DOMAIN, DEFINED BY THE SMHI PRODUCTION AREA “EURON1”. SEE FIGURE 8 AND FIGURE 9...	27
TABLE 5: VALIDATION SCORES FOR THE COLLOCATIONS OF GLOBAL SYNOP REPORTS WITH THE INTERMITTENT 2-YEAR DATASET OF PPS CLOUDMASK ON AVHRR AND VIIRS FROM LOCALLY RECEIVED SUOMI NPP, NOAA-18 AND NOAA-19 DATA.....	28
TABLE 6 ACCURACY MEASURES AND VERIFICATION SCORES FOR THE PPS CLOUD MASK (VERSION 2014) FOR LOCALLY RECEIVED S-NPP AND NOAA-18/19 DATA OVER EUROPE AND ARCTIC AS COMPARED TO CALIPSO. CALIPSO DATA FOR THE FILTERED CASE ARE FILTERED SO THAT PIXELS WITH TOTAL OPTICAL THICKNESS BELOW 0.2 (IN THE 5KM DATA SET, THIS INFORMATION IS NOT AVAILABLE IN THE 1KM DATA SET) ARE NOT CONSIDERED. SHOWN ARE THE OBSERVED ACCURACIES, TOTAL AND ALSO DIVIDED BY ILLUMINATION CONDITIONS, AS WELL AS THE REQUIRED ACCURACIES. HR DENOTES THE HIT RATE AND N THE NUMBER OF MATCHING PIXELS. GREEN: WITHIN TARGET ACCURACY. RED: NOT REACHING THRESHOLD ACCURACY.	29
TABLE 7 ACCURACY MEASURES AND VERIFICATION SCORES FOR THE PPS CLOUD MASK (VERSION 2014) FOR AVHRR-GAC DATA AS COMPARED TO CALIPSO. CALIPSO DATA FOR THE FILTERED CASE ARE HERE FILTERED SO THAT PIXELS WITH TOTAL OPTICAL THICKNESS BELOW 0.2 ARE CONSIDERED CLEAR. AS A REFERENCE THE SAME DATA SET FROM CLARA-A1 (PPS v2010) IS INCLUDED. SHOWN ARE THE OBSERVED ACCURACIES, TOTAL AND ALSO DIVIDED BY ILLUMINATION CONDITIONS, AS WELL AS THE REQUIRED ACCURACIES FOR SYNOP MATCHES. HR DENOTES THE HIT RATE AND N THE NUMBER OF MATCHING PIXELS. GREEN: WITHIN TARGET ACCURACY. LIGHT GREEN: ALSO WITHIN TARGET ACCURACY. RED: NOT REACHING THRESHOLD ACCURACY.	29
TABLE 8: RELATIVE AND ABSOLUTE FRACTION OF DIFFERENT CLOUD-CLASSES (DISTINGUISHED HERE BY CLOUD HEIGHT). PRESENTED ARE RESULTS FOR LOCALLY RECEIVED DATA OVER EUROPE AND ARCTIC AND AVHRR GAC DATA. THE COMPARISONS ARE NOT STRAIGHTFORWARD, BECAUSE ONLY PPS HAS THE CLASS ‘FRACTIONAL CLOUDS’. FROM THIS CLASS, THE MAJORITY OF FRACTIONAL CLOUDS ARE IN FACT LOW-LEVEL FRACTIONAL CLOUDS. ‘RELATIVE’ REFERS TO ‘FRACTION OF DETECTED CLOUDS’ AND ‘ABSOLUTE’ TO ‘FRACTION OF ALL PIXELS’.....	31
TABLE 9: BASIC ACCURACY DESCRIPTORS FOR THE CLOUD CLASSES: LOW, MEDIUM AND HIGH. THE ‘BC RMS’ DENOTES THE BIAS CORRECTED RMS AND HR THE HIT RATE. GREEN: WITHIN TARGET ACCURACY RED: NOT REACHING THRESHOLD ACCURACY. PRESENTED ARE RESULTS FOR LOCALLY RECEIVED DATA OVER EUROPE AND ARCTIC AND FOR AVHRR GAC DATA.	31
TABLE 10: A BASIC DESCRIPTION FOR THE COMPARISON OF THE PPS CLOUD TOP HEIGHT AND THAT, DERIVED BY CALIOP. DATA CONSIDERED IS LOCALLY RECEIVED DATA OVER EUROPE AND ARCTIC. GIVEN ARE TOTAL RESULTS AS WELL AS RESULTS SEPARATED IN DAY/NIGHT/TWILIGHT. IN THE FILTERED DATA: AS CLOUD TOP OF CALIOP IS USED THE HEIGHT AT 1.0 OPTICAL DEPTH DOWN IN THE CLOUD.....	34
TABLE 11: OBSERVED AND REQUIRED ACCURACIES FOR THE CLOUD TOP HEIGHTS FOR LOCALLY RECEIVED DATA OVER EUROPE AND ARCTIC. GREEN: WITHIN TARGET ACCURACY. LIGHT GREEN: ALSO WITHIN TARGET ACCURACY. RED: NOT WITHIN THRESHOLD ACCURACY. FOR THE SEMI-TRANSPARENT AND OPAQUE CLOUDS TOGETHER THE BIAS IS: -1100M, THE RMS IS 2535M AND BC-RMS 2284M (UNFILTERED CALIOP DATA).	36
TABLE 12 RETRIEVAL RATE FOR PGE03 FOR PPS VERSION 2014 COMPARE TO VERSION PPS v 2012 OR v2010.....	38
TABLE 13 OBSERVED AND REQUIRED ACCURACIES FOR THE CLOUD TOP HEIGHTS FOR AVHRR GAC DATA. GREEN: WITHIN THRESHOLD ACCURACY. LIGHT GREEN: ALSO WITHIN TARGET ACCURACY. RED: NOT WITHIN THRESHOLD ACCURACY. SEMI-TRANSPARENT AND OPAQUE RESULTS ARE PRESENTED TOGETHER. INCLUDED ARE FOR COMPARISON RESULTS FOR THE SAME ORBITS FROM CLARA-A1 (PPS v2010).	39
TABLE 14: CLOUD TOP HEIGHTS FOR LOCALLY RECEIVED DATA OVER EUROPE AND ARCTIC. COMPARING USING DEFAULT AND USING ACTUAL SURFACE EMISSIVITY AS INPUT TO RTTOV. RESULTS ARE FILTERED.....	42
TABLE 15: SUCCESS MATRIX FOR INDIVIDUAL MONTHS.	45

TABLE 16: SUCCESS MEASURES FOR INDIVIDUAL MONTHS. FOR VERSION 2014 VALUES ARE FOR ALL SOLAR ZENITH ANGLES. NUMBERS IN BRACKETS ARE FROM THE VALIDATION OF VERSION 2012, WHICH ONLY WERE DURING DAYTIME (SOLAR ZENITH ANGLE BELOW 72°) [RD.3.].....	46
TABLE 17: SUCCESS MATRIX FOR DAY AND NIGHT.	47
TABLE 18: SUCCESS MEASURES FOR DAY AND NIGHT.	47
TABLE 19: SUCCESS MATRIX FOR THE COMPLETE DATA SET.	48
TABLE 20: SUCCESS MEASURES FOR COMPLETE DATASET AND ACCORDING REQUIREMENTS.	48
TABLE 21: SUCCESS MATRIX FOR THE GAC DATA SET.	49
TABLE 22: SUCCESS MEASURES FOR GAC DATASET AND ACCORDING REQUIREMENTS.	50
TABLE 23: ACHIEVED ACCURACY (VALUES FOR VERSION 2012 IN BRACKETS) AND REQUIREMENTS FOR LWP PRODUCT.	55
TABLE 24: ACHIEVED ACCURACY (VALUES FOR VERSION 2012 IN BRACKETS) AND REQUIREMENTS FOR LWP PRODUCT IN DIFFERENT ILLUMINATION.	57
TABLE 25: REQUIRED AND ACHIEVED ACCURACIES FOR THE GLOBAL VALIDATION ACTIVITIES.	59
TABLE 26: OVERVIEW: STATISTICAL VALUES FOR THE INTERCOMPARISON OF MODIS AND PPS LWP PRODUCT.	63
FIGURE 1: GLOBAL MAP SHOWING THE LOCATION AND FREQUENCY OF ALL AVHRR GAC AND SYNOP COLOCATIONS, BASED ON THE 99 GAC ORBITS COVERING THE YEARS 2006 TO 2009.	14
FIGURE 2: GEOGRAPHICAL DISTRIBUTION OF COLLOCATED SYNOP STATIONS FOR THE DATA SET OF LOCALLY RECEIVED SUOMI NPP AND NOAA18&19.	15
FIGURE 3: NUMBER OF VIIRS/AVHRR-SYNOP COLOCATIONS OVER TIME, FOR THE DATASET OF LOCALLY RECEIVED SUOMI NPP, NOAA18 AND NOAA19 DATA.	16
FIGURE 4: EQUATORIAL CROSSING TIMES OF THE NOAA AND METOP SPACECRAFTS FROM NOAA-7 TILL TODAY'S NOAA-19 AND METOP-B.....	17
FIGURE 5: DISTRIBUTION IN TERMS OF SATELLITE ZENITH (UPPER PANEL), SUN ZENITH ANGLE (MIDDLE PANEL) AND TIME DIFFERENCE (LOWER PANEL) OF CALIPSO-VIIRS/AVHRR COLOCATIONS FROM NOAA-18, NOAA-19 AND SUOMI NPP. OBSERVATIONS SPAN NIGHT AND DAY WITH A PEAK OF OBSERVATIONS IN TWILIGHT AND NIGHTTIME, AND WITH THE MAJORITY OF OBSERVATIONS HAVING A NEAR NADIR (AVHRR/VIIRS) VIEW.	18
FIGURE 6: DISTRIBUTION IN TERMS OF SATELLITE ZENITH (UPPER PANEL), SUN ZENITH ANGLE (MIDDLE PANEL) AND TIME DIFFERENCE (LOWER PANEL) OF CALIPSO-AVHRR COLOCATIONS FROM THE 2006-2009 NOAA-18 GAC DATA RECORD. OBSERVATIONS SPAN NIGHT AND DAY WITH AN ALMOST FLAT DISTRIBUTION OVER NIGHT, TWILIGHT AND DAY, AND WITH THE MAJORITY OF OBSERVATIONS HAVING A NEAR NADIR AVHRR VIEW.....	19
FIGURE 7: GEOGRAPHICAL DISTRIBUTION OF SYNOP/AVHRR GAC COLOCATIONS IN TWILIGHT CONDITIONS (SUN ZENITH ANGLES BETWEEN 80 AND 95 DEGREES).	25
FIGURE 8: A QUICKLOOK OF THE USGS LANDUSE OVER THE SMHI PRODUCTION AREA 'EURON1', WHICH WE HAVE USED HERE TO FILTER THE SYNOP COLOCATIONS ACCORDING TO GEOGRAPHICAL LOCATION.	25
FIGURE 9: ALL SYNOP/AVHRR GAC COLOCATIONS WITHIN IN THE AREA DEFINED BY 'EURON1' (SEE FIGURE 8) CORRESPONDING TO NORTHERN EUROPE AND ADJACENT SEAS.	26
FIGURE 10 CLOUD TOP HEIGHTS FROM CALIPSO (TOP EDGE OF GREEN AREA) AND PPS ON VIIRS (BLUE) FOR ONE SWATH WHERE PPS PERFORMED POORLY FOR UNFILTERED DATA (LEFT) AND BETTER FOR FILTERED DATA (RIGHT). THIS IS DUE TO OPTICALLY THIN CLOUDS IN THE TOP LAYER. PPS IS NOT CAPTURING ACCURATE CLOUD TOP HEIGHT FROM A MULTIPLE CLOUD LAYER SCENE (TRACK POSITION 500-1000). IN THIS SWATH ALMOST ALL THE HIGH CLOUDS WERE OPTICALLY THIN (<1.0), AND THIS IS WHY SO MUCH OF THEM IS REMOVED IN THE FILTERING. THE LOW OPAQUE CLOUDS ARE OPTICALLY MUCH THICKER AND THE FILTERING DOES NOT REMOVE MUCH OF THESE. THE SWATH IS FROM 2012 OCTOBER 4:TH AT AROUND 7:AM, ORBIT NUMBER 4851. AND THE BLACK LAND TO THE RIGHT IN THE PICTURE IS GREENLAND.	40
FIGURE 11 EXAMPLE OF CMA AND CTTH OF A METOP GRANULE, 2013 16:TH JUNE, AT 03:34. NOTICE THAT MOST CLOUDS IN THE CLOUDMASK HAVE HEIGHTS IN THE CTTH.	41
FIGURE 12: GEOGRAPHICAL DISTRIBUTION OF MEASUREMENTS CONSIDERED FOR THIS INTER-COMPARISON. VALID IS THE NEAREST AVHRR PIXEL WITHIN 1KM RADIUS TO THE CALIOP PIXEL CENTRE IF THE QUALITY OF THE CALIOP PRODUCT IS NOT FLAGGED AS POOR QUALITY (NOTE THAT DIFFERENT PRODUCTS HAVE DIFFERENT QUALITY FLAGS. THEREFORE GEOGRAPHICAL DISTRIBUTION MAY VARY WITH CLOUD PRODUCT).	44
FIGURE 13: DISTRIBUTION AND LOCATION OF MEASUREMENT POINTS FOR THE YEAR UNDER INVESTIGATION (2010). UPPER LEFT JANUARY, UPPER RIGHT: APRIL, LOWER LEFT JULY AND LOWER RIGHT OCTOBER.....	45

FIGURE 14: DISTRIBUTION AND LOCATION OF MEASUREMENT POINTS SEPARATED BY ILLUMINATION CONDITIONS. DAY (SOLAR ZENITH ANGLE BELOW 72°) LEFT AND NIGHT (SOLAR ZENITH ANGLE ABOVE 72°) TO THE RIGHT.47

FIGURE 15: GEOGRAPHICAL DISTRIBUTION OF THE MATCHES BETWEEN CALIOP PIXELS AND GAC PIXELS FOR THE CPP CLOUD PHASE PRODUCT).49

FIGURE 16: **SPATIAL FREQUENCY DISTRIBUTION OF USED AMSR-E PIXEL. MATCHING CONDITIONS WERE EXTENDED TO: NO LAND PIXELS, NO ICE PHASE IN FOOTPRINT (ACCORDING TO THE CPP PRODUCT), AMSR-E LWP BETWEEN 0 AND 170 G/M² AND CPP LWP > 0 G/M².**52

FIGURE 17: **SPATIAL DISTRIBUTION OF OBSERVATIONS BY MONTH. UPPER LEFT: JANUARY, UPPER RIGHT: APRIL, LOWER LEFT: JULY AND LOWER RIGHT OCTOBER. NOTE: SOLAR ZENITH ANGLE IS RESTRICTED TO 72° (AS IN PREVIOUS INVESTIGATIONS FOR VERSION 2012).**53

FIGURE 18: **SCATTERING-DENSITY PLOTS SPLIT BY MONTH. THE COLOUR MARKS THE DENSITY OF HITS IN THE PLOTTED SPACE. UPPER LEFT: JANUARY, UPPER RIGHT: APRIL, LOWER LEFT: JULY AND LOWER RIGHT OCTOBER. THE CPP VALUES HERE ARE DISPLAYED ONLY UP TO A VALUE OF 170 G/M². AN EXAMPLE FOR THE WHOLE DATASET IN FULL RANGE IS SHOWN IN.....**54

FIGURE 19: **HISTOGRAMS OF DEVIATION CPP – AMSR-E. IN THIS SENSE ‘MEAN’ IS EQUAL TO THE ERROR DESCRIPTION BIAS AND ‘STD’ IS EQUAL TO THE BC RMS ERROR. TO KEEP FOCUS ON IMPORTANT FEATURES, THIS AND THE FOLLOWING DEVIATION HISTOGRAMS SHOW DATA BETWEEN THE 1 AND 99 PERCENTILE ONLY. UPPER LEFT: JANUARY, UPPER RIGHT: APRIL, LOWER LEFT: JULY AND LOWER RIGHT OCTOBER.**.....55

FIGURE 20: SCATTERING DENSITY (LEFT COLUMN) AND HISTOGRAM DEVIATIONS (RIGHT COLUMN) FOR ONLY DAYTIME PIXELS (SOLAR ZENITH ANGLE BELOW 72°, UPPER ROW) AND ENTIRE DATASET (SOLAR ZENITH ANGLE UP TO 84°, LOWER ROW). NOTE THE DIFFERENT SCALING FOR HISTOGRAMS IN RIGHT COLUMN.56

FIGURE 21: DATA-COVERAGE OF GLOBAL GAC-AMSR MATCHES. A TOTAL OF 1108330 COLLOCATED DATA POINTS MET THE REQUIREMENTS FOR THIS STUDY.58

FIGURE 22: SCATTERING DENSITY DIAGRAM OF AMSR-E LWP PRODUCT AND CPP LWP PRODUCT.59

FIGURE 23: PROBABILITY DENSITY FUNCTION OF DIFFERENCES BETWEEN PPS LWP PRODUCT AND AMSR-E LWP PRODUCT. THE VERTICAL DOTTED LINE MARKS THE BIAS (29.5 G/M²) WHILE THE HORIZONTAL DOTTED LINE ILLUSTRATES THE RMS DEVIATIONS (96.5 G/M²).60


FIGURE 24: GLOBAL DISTRIBUTION OF PPS - MODIS MATCHES FOR THE SELECTED GAC SCENES. THE TOTAL NUMBER OF COLLOCATED PIXEL IS 838851.61

FIGURE 25: SCATTERING DENSITY (LEFT) AND PROBABILITY DENSITY OF DEVIATIONS (RIGHT) FOR PPS – MODIS MATCHES. ADDITIONALLY, THE RIGHT IMAGE PROVIDES INFORMATION ABOUT THE BIAS (VERTICAL DOTTED LINE, HERE 49.0 G/M²) AND THE RMS DEVIATION (HORIZONTAL DOTTED LINE, HERE 246.2 G/M²).61

FIGURE 26: GLOBAL DISTRIBUTION OF PPS – MODIS MATCHES OVER SEA (LEFT) AND OVER LAND (RIGHT). IN TOTAL, 735752 OF THE SELECTED PIXEL ARE OVER SEA AND 103099 ARE OVER LAND.62

FIGURE 27: SAME AS FIGURE 25 BUT ONLY SEA PIXELS ARE CONSIDERED. THE BIAS HERE IS 52.6 G/M² AND THE RMS DEVIATION IS 242.0 G/M².62

FIGURE 28: SAME AS FIGURE 25 BUT ONLY FOR PIXELS OVER LAND. HERE THE BIAS IS 23.6 G/M² AND THE RMS DEVIATION IS GIVEN WITH 273.2 G/M².63

	Scientific and Validation Report for the Cloud Product Processors of the NWC/PPS	Code: NWC/CDOP2/PPS/SMHI/SCI/VR/Cloud Issue: 1.0 Date: 15 September 2014 File: NWC-CDOP2-PPS-SMHI-SCI-VR-Cloud_v1_0 Page: 8/67
--	--	--

1 INTRODUCTION

The EUMETSAT “Satellite Application Facilities” (SAF) are dedicated centres of excellence for processing satellite data, and form an integral part of the distributed EUMETSAT Application Ground Segment (<http://www.eumetsat.int>). This documentation is provided by the SAF on Support to Nowcasting and Very Short Range Forecasting, SAFNWC. The main objective of SAFNWC is to provide, further develop and maintain software packages to be used for Nowcasting applications of operational meteorological satellite data by National Meteorological Services. More information can be found at the SAFNWC webpage, <http://www.nwcsaf.org> . This document is applicable to the SAFNWC processing package for polar orbiting meteorological satellites, SAFNWC/PPS, developed and maintained by SMHI (<http://nwcsaf.smhi.se>).

1.1 PURPOSE

This document is a report presenting validations results of the cloud products from NWC/SAF. The threshold, target and optimal accuracies validated against are described in the Product Requirement Document [AD.4.].

1.2 SCOPE

This document presents the validation result of the NWC/SAF cloud products: PGE01 version 4.0, PGE02 version 2.0, PGE03 version 4.0 and PGE05 version 1.1 - all applicable to PPS version 2014.

1.3 DEFINITIONS AND ACRONYMS

<i>EUMETSAT Satellite Application Facility to NoWcasting & Very Short Range Forecasting</i>	Scientific and Validation Report for the Cloud Product Processors of the NWC/PPS	Code: NWC/CDOP2/PPS/SMHI/SCI/VR/Cloud Issue: 1.0 Date: 15 September 2014 File: NWC-CDOP2-PPS-SMHI-SCI-VR-Cloud_v1_0 Page: 9/67
---	--	--

Acronym	Explanation	Acronym	Explanation
ACPG	AVHRR/AMSU Cloud Product Generation software (A major part of the SAFNWC/PPS s.w., including the PGE:s.)	EUMETSAT	European Organisation for the Exploitation of Meteorological Satellites
AEMET	Agencia Estatal de Meteorología (Spain)	GEO	
AHAMAP	AMSU-HIRS-AVHRR Mapping Library (A part of the SAFNWC/PPS s.w.)	MHS	Microwave Humidity Sounding Unit
AMSU	Advance Microwave Sounding Unit	NOAA	National Oceanic and Atmospheric Administration
AVHRR	Advanced Very High Resolution Radiometer	PC	Precipitating Cloud (also PGE04)
CDOP	Continuous Development and Operational Phase	PGE	Process Generating Element
CDOP-2	Second Continuous Development and Operational Phase	PPS	Polar Platform System
CMA	Cloud Mask (also PGE01)	SAF	Satellite Application Facility
CPP	Cloud Physical Products	SAFNWC	Satellite Application Facility for support to NoWcasting
CT	Cloud Type (also PGE02)	SMHI	Swedish Meteorological and Hydrological Institute
CTTH	Cloud Top Temperature, Height and Pressure (also PGE03)	TBC	To Be Confirmed
EPS	EUMETSAT Polar System	TBD	To Be Defined
		VIIRS	Visible Infrared Imaging Radiometer Suite

See [RD.1.] for a complete list of acronyms for the SAFNWC project.

1.4 REFERENCES

1.4.1 Applicable documents

The following documents, of the exact issue shown, form part of this document to the extent specified herein. Applicable documents are those referenced in the Contract or approved by the Approval Authority. They are referenced in this document in the form [AD.X]

For dated references, subsequent amendments to, or revisions of, any of these publications do not apply. For undated references, the current edition of the document referred applies.

Current documentation can be found at SAFNWC Helpdesk web: <http://www.nwcsaf.org>

<i>EUMETSAT Satellite Application Facility to NoWCASTing & Very Short Range Forecasting</i>	Scientific and Validation Report for the Cloud Product Processors of the NWC/PPS	Code: NWC/CDOP2/PPS/SMHI/SCI/VR/Cloud Issue: 1.0 Date: 15 September 2014 File: NWC-CDOP2-PPS-SMHI-SCI-VR-Cloud_v1_0 Page: 10/67
---	--	---

Ref	Title	Code	Vers	Date
[AD.1.]	Proposal for the Second Continuous Development and Operations Phase (CDOP) March 2012 – February 2017	NWC/CDOP2/MGT/AEMET/PRO	1.0	15/03/11
[AD.2.]	NWCSAF Project Plan	NWC/CDOP2/SAF/AEMET/MGT/PP	1.5	05/06/14
[AD.3.]	Software Verification and Validation Plan for the SAFNWC/PPS	NWC/CDOP2/PPS/SMHI/MGT/SVVP	1.0	15/09/14
[AD.4.]	NWCSAF Product Requirements Document	NWC/CDOP2/SAF/AEMET/MGT/PRD	1.5	05/06/14
[AD.5.]	System and Components Requirements Document for the SAFNWC/PPS	NWC/CDOP2/PPS/SMHI/SW/SCRD	1.0	15/09/14

Table 1: List of Applicable Documents

1.4.2 Reference documents

The reference documents contain useful information related to the subject of the project. These reference documents complement the applicable ones, and can be looked up to enhance the information included in this document if it is desired. They are referenced in this document in the form [RD.X]

For dated references, subsequent amendments to, or revisions of, any of these publications do not apply. For undated references, the current edition of the document referred applies

Current documentation can be found at SAFNWC Helpdesk web: <http://www.nwcsaf.org>

Ref	Title	Code	Vers	Date
[RD.1.]	The Nowcasting SAF Glossary	NWC/CDOP2/SAF/AEMET/MGT/GLO		
[RD.2.]	Products Validation report for the SAFNWC/PPS version 2012	SAF/NWC/CDOP/SMHI-PPS/SCI/VR/7	2.4.1	16/04/12
[RD.3.]	Products Validation report for the SAFNWC/PPS CPP version 2012	SAF/NWC/CDOP/SMHI-PPS/SCI/VR/6	2.4.2	07/05/12
[RD.3b.]	Product Validation report for the SAFNWC/PPS version 2008 (and 2.0)	SAF/NWC/CDOP/SMHI-PPS/SCI/VR/1	2.1.1	19/03/08
[RD.4.]	NWCSAF Visiting Scientist report “Investigation of PPS CTH Using CALIPSO Validation Tool”, Chang-Hwan Park 2012			12/03/12
[RD.5]	Algorithm Theoretical Basis Document for the Cloud Mask of the NWC/PPS	NWC/CDOP2/PPS/SMHI/SCI/ATBD/1	1.0	15/09/14

Table 2: List of Referenced Documents

1.5 DOCUMENT OVERVIEW

This document contains the scientific validation results for NWCSAF PPS v2014. After this introduction follows section 2 which lists and defines the verification measures used through out the data analysis. Section 3 describes the satellite datasets and validation datasets (also happens to be satellite based) used and section 4 presents and discuss the results. Section 5 summarise and conclude, and a few scientific references cited are given in section 6. ANNEX A contains a list of still open TBCs and TBDs.

2 DEFINITION OF VERIFICATION MEASURES USED

In the following chapters we present the validation results using standard verification measures. Below we provide a short definition of each utilized, where ‘validating truth’ is the result of another product we are validating against. In the definitions below, we use cloud mask as an example, but the verification measures are applicable to additional PPS products.

We define N as the total number of observations, whereas A, B, C, and D are assigned numerical values based on statistical estimates described below.

	Validating truth Cloudy	Validating truth Cloud-free
PPS Cloudy	A	B
PPS Cloud-free	C	D

Bias:

$$\frac{1}{N} * \sum_k (y_k - o_k)$$

Where the sum is over all k data pairs of PPS cloud cover (y) and the validating truth cloud cover (o).

Root Mean Square Deviation (RMS):

$$\sqrt{\frac{1}{N} * \sum_k (y_k - o_k)^2}$$

Bias corrected Root Mean Square Deviation (bc RMS):

$$\sqrt{\frac{1}{N} * \sum_k (y_k - o_k - Bias)^2} = \sqrt{RMS^2 - Bias^2}$$

Hit rate (HR) also sometimes denoted PC (percent correct):

$$(A+D)/N$$

POD-cloudy:

$$A/(A+C)$$

<i>EUMETSAT Satellite Application Facility to NoWCasting & Very Short Range Forecasting</i>	Scientific and Validation Report for the Cloud Product Processors of the NWC/PPS	Code: NWC/CDOP2/PPS/SMHI/SCI/VR/Cloud Issue: 1.0 Date: 15 September 2014 File: NWC-CDOP2-PPS-SMHI-SCI-VR-Cloud_v1_0 Page: 12/67
---	--	---

FAR-cloudy:

$$B/(A+B)$$

POD-clear:

$$D/(B+D)$$

FAR-clear:

$$C/(C+D)$$

It has to be emphasized here that the set of statistical scores presented above are obviously not all independent. For instance, in the binary case (cloud mask validation) the hit rate (H) and the RMS are directly related through:

$$HR = 1 - RMS^2$$

This is because:

$$\begin{aligned}
 N * RMS^2 &= \sum_k (y_k - o_k)^2 \\
 &= C + B \\
 &= N - (A + D)
 \end{aligned}$$

Even though there usually is such a tight interconnection between the different statistical measures we will be using all of them in the following to emphasize different aspects of the validation results.

<i>EUMETSAT Satellite Application Facility to NoWCASTing & Very Short Range Forecasting</i>	Scientific and Validation Report for the Cloud Product Processors of the NWC/PPS	Code: NWC/CDOP2/PPS/SMHI/SCI/VR/Cloud Issue: 1.0 Date: 15 September 2014 File: NWC-CDOP2-PPS-SMHI-SCI-VR-Cloud_v1_0 Page: 13/67
---	--	---

3 DATA USED

3.1 THE VIIRS INSTRUMENT ONBOARD SUOMI NPP AND ITS DATA

The Suomi National Polar-orbiting Partnership (S-NPP) spacecraft was launched successfully in late October 2011. The largest of its five payloads is the Visible Infrared Imaging Radiometer Suite (VIIRS). This visible/infrared radiometer features 22 spectral bands with 0.371 km nadir resolution for the five imager resolution bands and 0.742 km nadir resolution for the Day/Night band and the moderate resolution bands.

To account for along-track distortions, overlapping pixels are removed (so called ‘Bowtie Removal’). Problems related to across-track distortions are avoided by pixel aggregation. The pixels are at nadir angle rather oblong and more quadratic at swath edges. Three oblong pixels close to nadir are aggregated into one more quadratic pixel. At the swath edge no pixels are aggregated, and in between two pixels are aggregated together. This makes the pixels more equally sized across the swath. As a positive side effect, the aggregation increases the signal to noise ratio.

For the processing of PPS cloud products, the AVHRR-heritage channels (0.6, 0.8, 1.6, 3.7, 11 and 12 microns) and the 8.5 micron channel in moderate resolution are used.

3.2 NWP DATA

For the validation forecasted NWP data from ECMWF is used. Data for all pressure levels available were included in the data: 91 levels up to 2013-06-30 and 137 levels after that.

For PGE01, PGE02 and PGE03 validation: Forecast lengths of 9-15h were used. Forecast valid times differed at most 1.5h from the time of the first scan line in the swath. No sea/ice information was included in the validation.

For PGE05 validation: Forecast lengths of 6-9h were used. Forecast valid times differed at most 6h (in most cases up to 3h), from the time of the first scan line in the swath. Sea/ice information was used for all the scenes, as well as NWP snow data.

For GAC data NWP analysis data from ERA-interim were used.

3.3 THE SYNOP DATA

The PPS cloudmask has been validated against global Synop reports, using both AVHRR GAC data and locally received AVHRR and VIIRS from the direct readout (DR) station in Norrköping, Sweden. The Synop data used have been acquired from DWD, and kindly provided by Martin Stengel and Anke Kniffka.

For the GAC data we have used a 6x6 GAC pixel window centred over the Synop station, and for the local full resolution data we have used 20x20 AVHRR or VIIRS M-band pixels. The time difference between the AVHRR/VIIRS pixel and the Synop report time is allowed to deviate by up to 30 minutes.

The geographical distribution of Satellite-Synop collocations based on the GAC dataset is shown in Figure 1. The distribution is global but there is an obvious concentration of Synop matchups in central and northern Europe, including Germany.

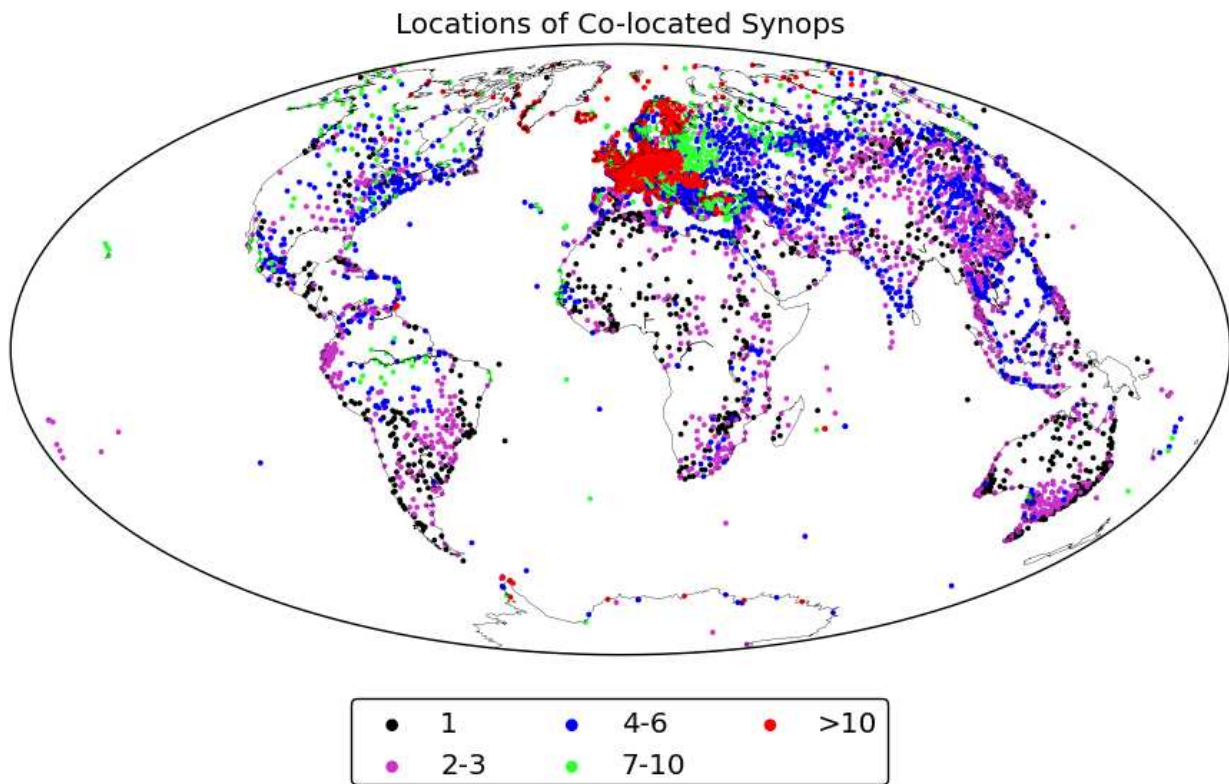


Figure 1: Global map showing the location and frequency of all AVHRR GAC and Synop co-locations, based on the 99 GAC orbits covering the years 2006 to 2009.

Figure 2 shows the collocations based on the DR data from Norrköping covering Europe. The density and geographical distribution is of course determined by the coverage of the DR data from the Norrköping station and the Synop report database acquired at DWD.

From the time histogram in Figure 3 we see that there are Synop collocations over the entire year from October 2012 to October 2013, however, with a small deficit of wintertime matchups and slight bias towards springtime.

Locations of Co-located Synops

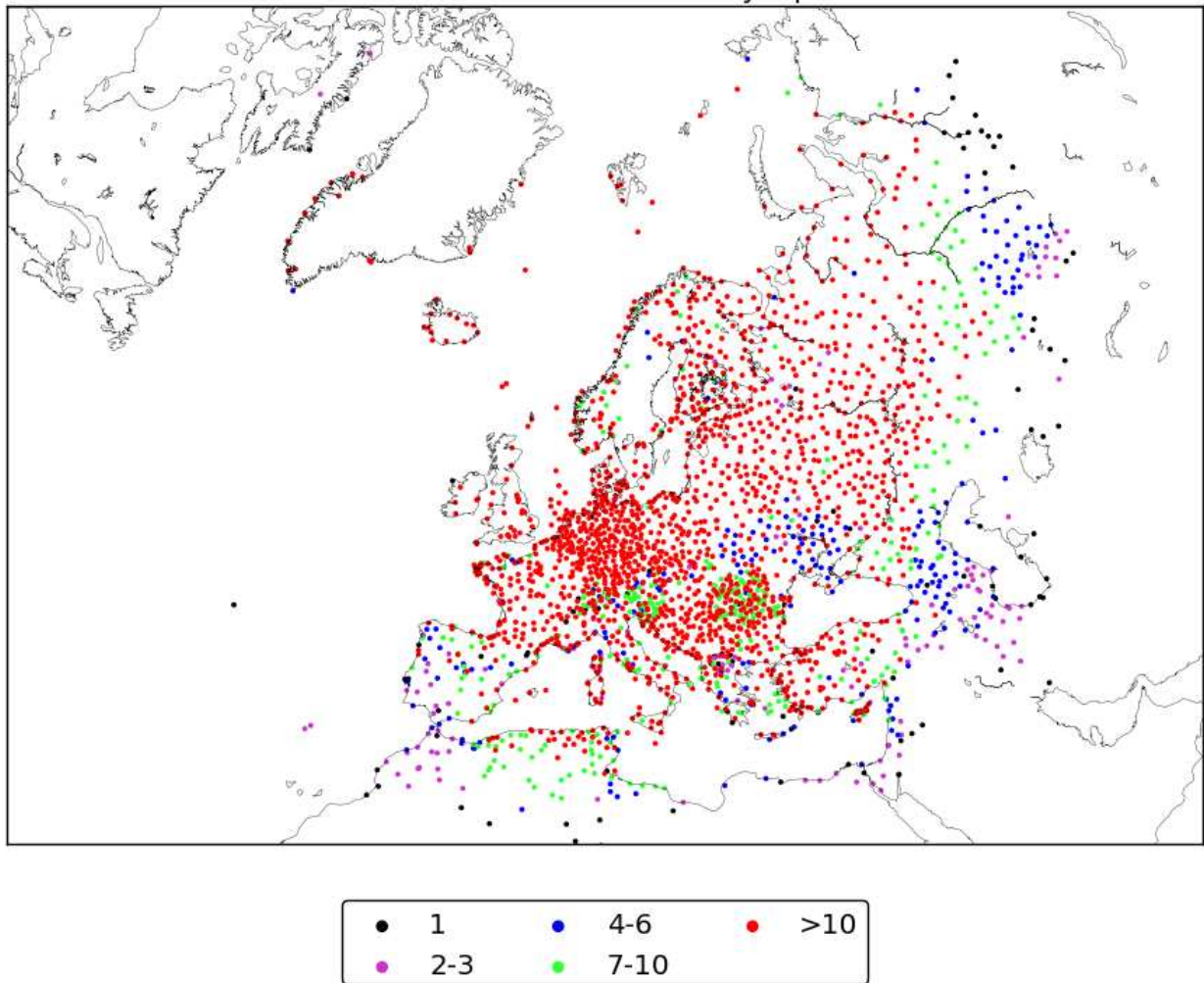


Figure 2: Geographical distribution of collocated Synop stations for the data set of locally received Suomi NPP and NOAA18&19.

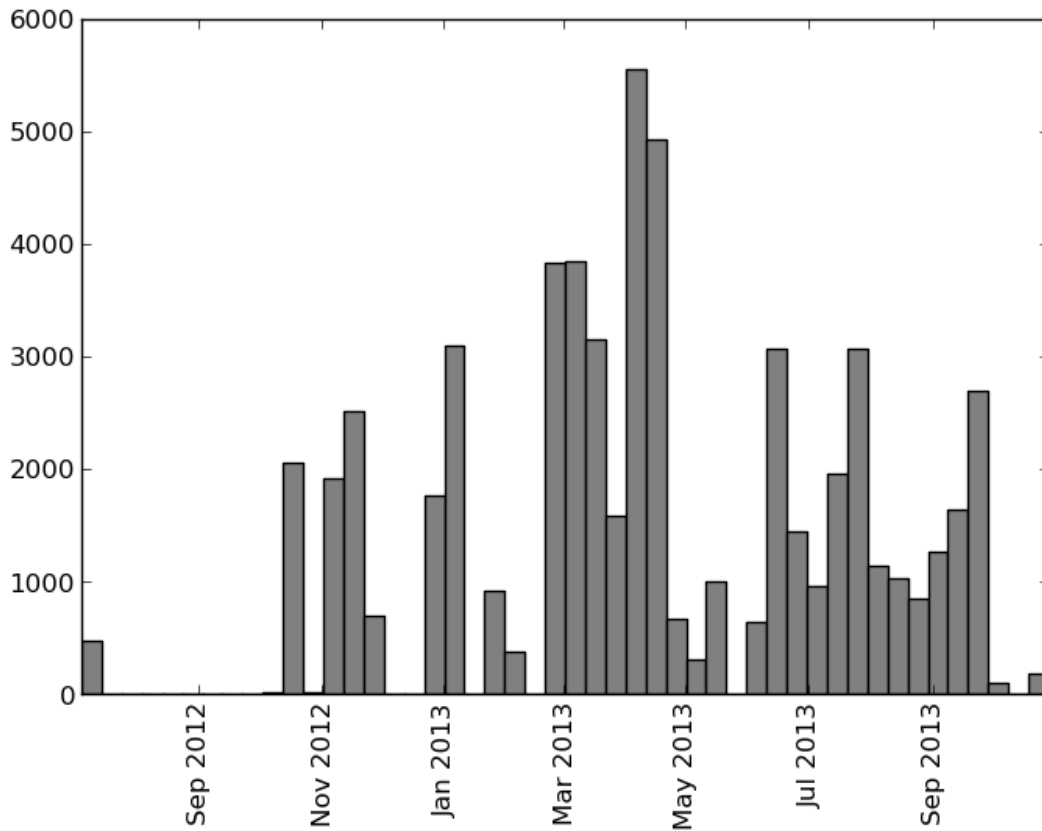
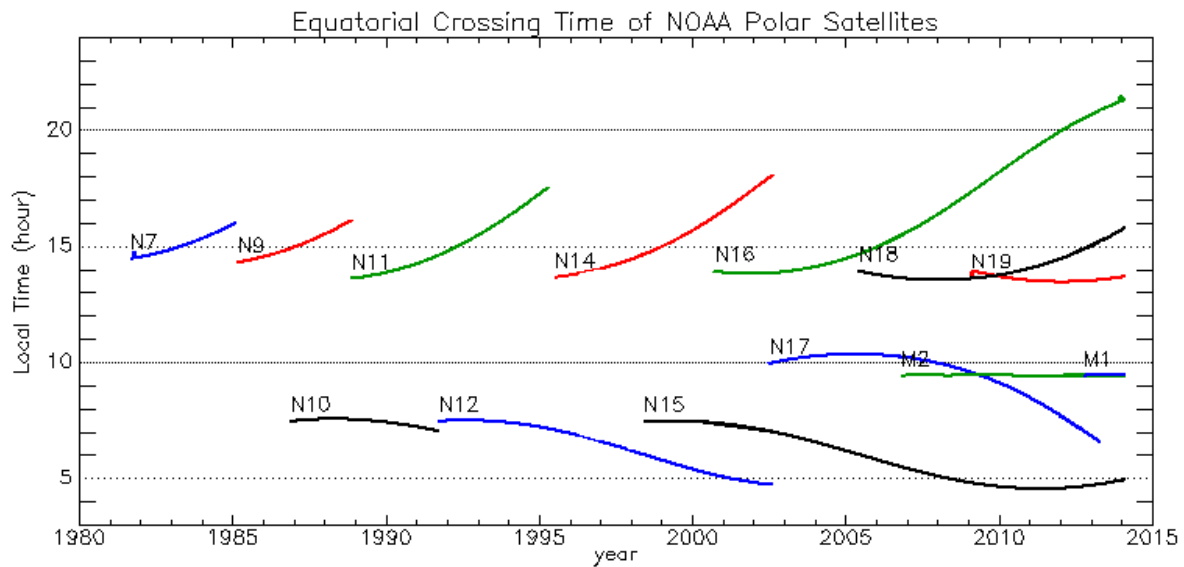


Figure 3: Number of VIIRS/AVHRR-Synop collocations over time, for the dataset of locally received Suomi NPP, NOAA18 and NOAA19 data.

3.4 THE CALIPSO DATABASE

Several active and passive satellite sensors are flying in a formation called the A-train. One satellite flying in the A-train is the Cloud-Aerosol Lidar and Infrared Pathfinder Satellite (CALIPSO) that was launched in April 2006. The CALIPSO payload consists of three nadir-viewing instruments: Cloud-Aerosol Lidar with Orthogonal Polarization (CALIOP), the imaging infrared radiometer (IIR), and the wide field camera (WFC). We have used data from the CALIOP instrument for the AVHRR/VIIRS-CALIPSO comparison presented in the study.

Fortunately, there is an overlap of both the VIIRS data record and the AVHRR data record with the data from CALIPSO. Though their orbits differ, the orbits of the three afternoon satellites Suomi NPP and NOAA18/19 do align periodically with the A-train formation. Where the Suomi NPP orbital plane is well maintained and stable over the lifetime of the satellite this is not the case with the NOAA satellites. However until around 2010 the NOAA-18 satellite orbit was rather well aligned with CALIPSO, and NOAA-19 is still today well aligned with CALIPSO. See plot of the equatorial crossing times in Figure 4.



Updated on 01/22/2014 04:13

Figure 4: Equatorial crossing times of the NOAA and Metop spacecrafts from NOAA-7 till today's NOAA-19 and Metop-B.

In this report we have investigated twelve months (June 2012 to May 2013) of matching Suomi NPP overpasses with CALIPSO observations. We have also included 59 scenes of matching NOAA18/19 and CALIPSO data. A match here is defined successful if observations at one position by both the Suomi NPP or NOAA18/19 and A-Train satellites were performed within a +/- 10 minute time-window. No correction for the parallax has been attempted, as the error introduced by ignoring the parallax effect is assumed small over this dataset. As can be seen from Figure 5 the AVHRR/VIIRS observations are if not close to nadir, then at least with rather low zenith angles, indicating that parallax effects should be relatively small on average. See also discussion below under co-location criteria.

The area expands to the coverage of overpasses received at the local X/L-band reception station at SMHI in Norrköping, which more or less equals the European and Arctic area. In total this results in 140 matching scenes for the months June 2012 to May 2013 for Suomi NPP and 60 matching scenes for NOAA18/19 for the months Mars 2013 to October 2013.

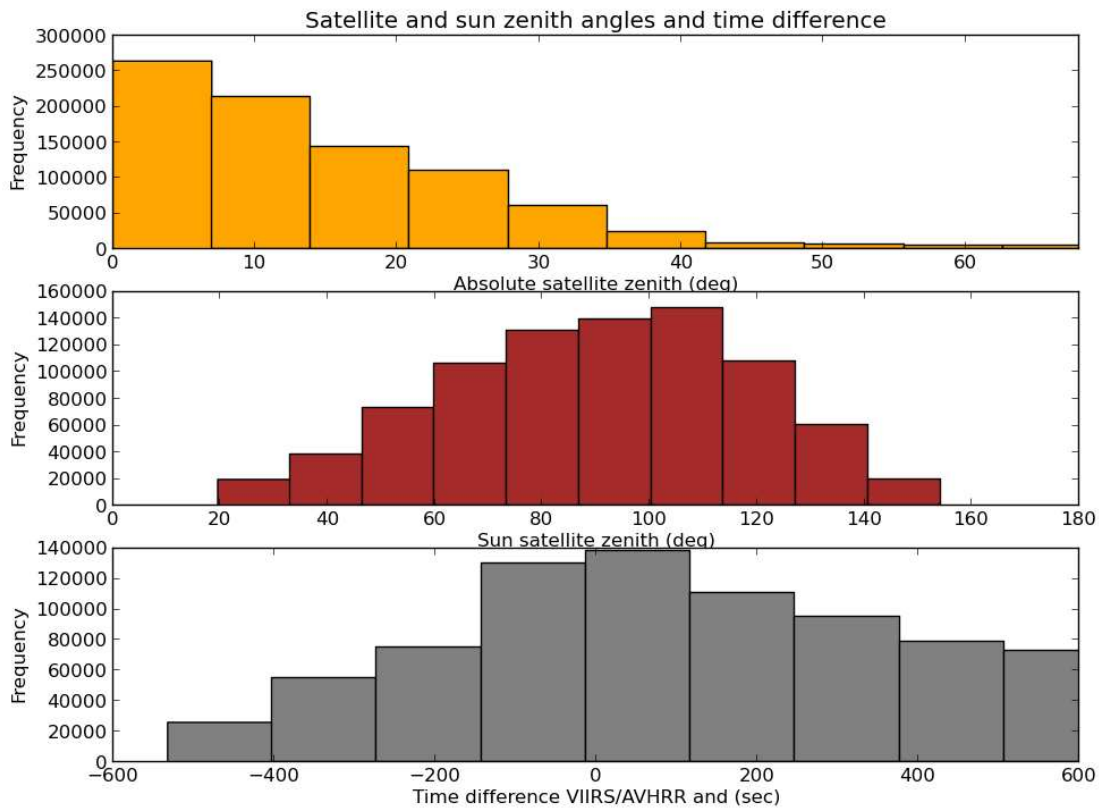


Figure 5: Distribution in terms of satellite zenith (uppr panel), sun zenith angle (middle panel) and time difference (lower panel) of CALIPSO-VIIRS/AVHRR collocations from NOAA-18, NOAA-19 and Suomi NPP. Observations span night and day with a peak of observations in twilight and nighttime, and with the majority of observations having a near nadir (AVHRR/VIIRS) view.

We have also matched and analyzed 99 GAC orbits of AVHRR18data, year 2006-2009, with CALIPSO data.

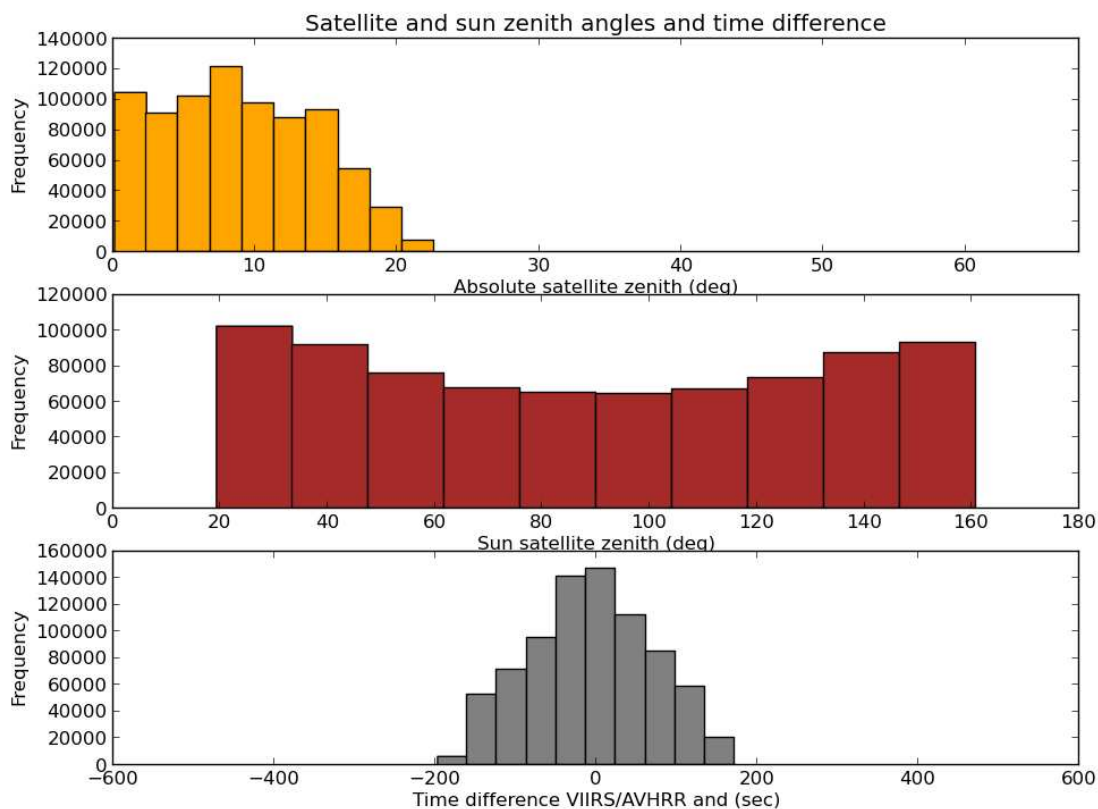


Figure 6: Distribution in terms of satellite zenith (upper panel), sun zenith angle (middle panel) and time difference (lower panel) of CALIPSO-AVHRR collocations from the 2006-2009 NOAA-18 GAC data record. Observations span night and day with an almost flat distribution over night, twilight and day, and with the majority of observations having a near nadir AVHRR view

For the locally received data we use the CALIOP Level 2 and 3 cloud layer data product from NASA Langley produced at 1km horizontal and 30m vertical resolution to quantify cloud fraction and cloud height (and some additional information from the 5km product for data filtering). For the GAC orbits we use mainly the 5km data, combined with information from the 1km data. (See Karlsson et. Johansson 2013). These data were obtained from the NASA Langley Research Center Atmospheric Science Data Center. More information on CALIPSO can be found at <http://www-CALIPSO.larc.nasa.gov/>. In the following we use the term CALIPSO synonymous with the CALIOP instrument on CALIPSO.

Technical details about the CALIOP 1km dataset:

Archive Center:

Atmospheric Science Data Center archive center details

Distributing Center:

* NASA Langley Research Center Atmospheric Science Data Center

* <http://eosweb.larc.nasa.gov>

<i>EUMETSAT Satellite Application Facility to NoWCASTing & Very Short Range Forecasting</i>	Scientific and Validation Report for the Cloud Product Processors of the NWC/PPS	Code: NWC/CDOP2/PPS/SMHI/SCI/VR/Cloud Issue: 1.0 Date: 15 September 2014 File: NWC-CDOP2-PPS-SMHI-SCI-VR-Cloud_v1_0 Page: 20/67
---	--	---

* Contacts

- o User Services
- o 757.864.8656 (BUSINESS)
- o larc@eos.nasa.gov

ShortName:

CAL_LID_L2_01kmCLay-ValStage1-V3-02

Version:

V3-02, V3-30

Description:

CALIPSO Lidar Level 2 1 km cloud layer data

Technical details about the CALIOP 5km dataset:

Archive Center:

Atmospheric Science Data Center archive center details

Distributing Center:

- * NASA Langley Research Center Atmospheric Science Data Center
- * <http://eosweb.larc.nasa.gov>
- * Contacts
 - o User Services
 - o 757.864.8656 (BUSINESS)
 - o larc@eos.nasa.gov

ShortName:

CAL_LID_L2_05kmCLay-Prov-V3-02

Version:

V3-02, V3-30

Description:

CALIPSO Lidar Level 2 5 km cloud layer data

Co-location criteria with VIIRS/AVHRR:

The CALIOP pixel is co-located with the nearest VIIRS/AVHRR pixel. Since CALIOP is a nadir viewing instrument with 333 m wide sampling, the VIIRS pixel in moderate resolution (which is used in general) and AVHRR pixel covers an area comparable to the aggregated 1 km CALIOP product. Remaining uncertainties are navigation uncertainties, typically of less than a pixel, and parallax effects for VIIRS/AVHRR, which are not being corrected for. The theoretical maximum displacement due to a VIIRS/VIIRS pixel for a 10 km high cloud at the outer part of the swath (which corresponds to a scan-angle as large as 56°) can be on the order of 15 km. However since NPP/NOAA and CALIPSO satellite ground track approximately coincide, a more typical displacement would be for a viewing angle of less than 10 degrees, and thus be below 2 km. All co-locations between VIIRS/AVHRR and CALIOP are made within a 20-min time window. Thus, any

<i>EUMETSAT Satellite Application Facility to NoWCasting & Very Short Range Forecasting</i>	Scientific and Validation Report for the Cloud Product Processors of the NWC/PPS	Code: NWC/CDOP2/PPS/SMHI/SCI/VR/Cloud Issue: 1.0 Date: 15 September 2014 File: NWC-CDOP2-PPS-SMHI-SCI-VR-Cloud_v1_0 Page: 21/67
---	--	---

VIIRS pixels with less than +/- 10-min separation from CALIPSO are retained and analyzed in the statistics below.

Adapt for geolocation inaccuracies:

In order to account for geolocation inaccuracies and deviations in colocations due to time of observation and instrument characteristics (different footprint patterns) CALIPSO cloud fraction is calculated as an average of the 1km CALIOP data, corresponding to three neighbouring VIIRS/AVHRR pixels along CALIOP track. For the resulting CALIPSO cloud fraction values, the following translation to clear and cloudy is used: CALIPSO cloud_fraction < 0.34 is taken as clear. CALIPSO cloud_fraction > 0.66 is taken as cloudy. This method is used for comparison with high resolution data only. For GAC the 5km CALIOP data are coinciding well with GAC resolution, and averaging over a 15km track would rather introduce additional errors.

Co-location criteria with AVHRR GAC:

Adapt for detectability differences – Optical depth filtering using 5km CALIPSO data:

Active (like CALIOP) and passive instruments (like VIIRS) feature different detectability of hydrometeors. This means that results are expected to differ dependent on which instruments data is considered regardless of the performance of the algorithm used. In short: differences between the validation truth and the PPS results are expected because there is systematic difference between the instruments.

The aim of this report is to validate the applied algorithm, not the instrument. Therefore, a filtering technique using some of the ideas described in Karlsson and Johansson (2013), is applied to filter CALIPSO data for the locally received data. Karlsson and Johansson, 2013, found that an optical thickness of 0.3 can be considered the average optical detection limit for PPS on AVHRR. In lack of other similar studies we currently regard this as the optical detection limit also for VIIRS data. Some more unpublished investigations have shown that the limit might be a bit lower and equal to 0.2. We will use 0.2 as the detection limit for AVHRR and VIIRS.

A detectable cloud height is retrieved from CALIPSO 5 km data in the following way: The optical thickness of a cloud layer in 5 km data is assumed to spread evenly over the 5 km spatial grid for that vertical layer. The profile height corresponding to an optical thickness of 1.0 is retrieved. The optical thickness value of 1 corresponds to findings of Minnis et al (2008), for the effective height of typical thick ice clouds. For the corresponding pixels in the 1 km CALIPSO data, the upper (undetectable) part of the cloud is ignored. Finally the PPS cloud top height is compared with the corrected (i.e. lower) cloud top height from CALIOP.

The optical thickness filtering of 1.0 is not universal. The goal with the filtering is to allow for a fairer comparison, because we compare the PPS cloud height to the CALIOP cloud height it is likely to be able to detect. However regarding clouds with a total optical thickness below 1.0 it is more difficult to know what is best to do. In some cases PPS is not able to detect these clouds, but sometimes they are detected. Thus we do not wish to completely remove these clouds, even though PPS most likely can not “see” many of them, because they are optically too thin. The reference CALIOP cloud top for these clouds is set to cloud base plus 100m. In the report both filtered and unfiltered results are presented.

The optical thickness information is also used to divide height data into two categories: thick top layer and thin top layer. Thick pixels are where the top layer has an optical thickness above detection

<i>EUMETSAT Satellite Application Facility to NoWCASTing & Very Short Range Forecasting</i>	Scientific and Validation Report for the Cloud Product Processors of the NWC/PPS	Code: NWC/CDOP2/PPS/SMHI/SCI/VR/Cloud Issue: 1.0 Date: 15 September 2014 File: NWC-CDOP2-PPS-SMHI-SCI-VR-Cloud_v1_0 Page: 22/67
---	--	---

limit (0.2) and thin pixels where the top layer has an optical thickness below detection limit. This separation is not perfect either but most of the actually very thin clouds will end up in the thin category. And most of the thicker clouds will end up in the thicker category.

The optical thickness information is also used to filter results for cloudmask. Pixels with optical thickness below 0.2 are for that case not considered. They could have been treated as clear. However the optical thickness information is only present on 5km resolution. There would be a risk that geographically small clouds that are quite optically thick would be considered clear.

3.5 THE AMSR-E DATA SET

For this study the LWP product of the Advanced Microwave Scanning Radiometer for EOS (AMSR-E) onboard the AQUA platform has been used to provide an independent dataset to compare the CPP LWP against. The passive microwave measurements provided by AMSR-E provides a somewhat more direct means of estimating the LWP compared to what can be achieved by the VIIRS/AVHRR based CPP products. The coarse spatial resolution of the AMSR-E channels and other obvious limitations mentioned later (see 4.4.2) is of course an important limiting factor searching for a method to validate the CPP LWP product. The AMSR-E data does not provide any ground truth.

Technical details about the AMSR-E dataset:

Archive Center:

NSIDC archive center details

Distributing Center:

- * NSIDC National Snow and Ice Data Center
- * <http://nsidc.org>
- * Contacts
 - o NSIDC DAAC User Services
 - o +1 303-492-6199 (BUSINESS)
 - o nsidc@nsidc.org

ShortName:

AE_Ocean

Version:

2

Description:

The AMSR-E/Aqua Level-2B ocean product includes Sea Surface Temperature at 56 and 38 km, near-surface wind speed at 38 and 21 km, columnar water vapor at 21 km, and columnar cloud liquid water at 12 km, generated by the Wentz algorithm using Level-2A TBs.

3.6 THE MODIS LWP DATA SET

In the search for means to validate the CPP LWP product, especially over land where the AMSR-E dataset presented above is not useful, we have chosen to make an intercomparison of the CPP LWP with the corresponding official product from the MODIS team at NASA Langley. See 4.4.2.4 for the outcome of this study and further details on the data and method.

<i>EUMETSAT Satellite Application Facility to NoWcasting & Very Short Range Forecasting</i>	Scientific and Validation Report for the Cloud Product Processors of the NWC/PPS	Code: NWC/CDOP2/PPS/SMHI/SCI/VR/Cloud Issue: 1.0 Date: 15 September 2014 File: NWC-CDOP2-PPS-SMHI-SCI-VR-Cloud_v1_0 Page: 23/67
---	--	---

Technical details about the MODIS LWP dataset:

Archive Center:

LAADS archive center details

Distributing Center:

* LAADS Level 1 and Atmosphere Archive and Distribution System

* <http://ladsweb.nascom.nasa.gov>

* Contacts

o MODAPS User Support

o + 1-866-506-6347

o modapsuso@sigmaspace.com

ShortName:

MYD06_L2

Version:

Collection 6

Description:

Aqua Atmosphere Level 2 Cloud product. Standard waterpath subset.

4 RESULTS AND DISCUSSION

In this section, the comparison results are shown separated by cloud product (cloud mask, cloud type and cloud top temperature and height, and cloud physical properties).

4.1 CLOUD MASK

4.1.1 Synop validation

The results of the global validation using the archive of 99 GAC orbits are presented below in Table 3. For all sun illuminations (first row) the data corresponds to the colocations shown in Figure 1. The data are also stratified according to sun illumination. See [RD.5] for the definition of day, night and twilight. It is worthwhile noticing that the dataset is relatively small for twilight cases in particular, and that twilight corresponds to high latitude Arctic and Antarctic conditions. See plot in Figure 7.

Table 3 Validation scores for 99 GAC orbits against global Synop reports

Observed Accuracy									
	RMS	MAE	Hit rate	Bias (%)	Pod cloudy	Far cloudy	Pod clear	Far clear	N
All	2.26	1.49	0.901	0.41	0.935	0.058	0.765	0.260	20298
Day	1.96	1.31	0.933	-0.62	0.950	0.030	0.845	0.238	12861
Night	2.77	1.83	0.841	4.01	0.908	0.123	0.667	0.265	5966
Twilight	2.58	1.71	0.870	-4.56	0.896	0.055	0.746	0.403	1471
Target Accuracy (globally)									
	MAE	Hit rate	Bias (%)	Pod cloudy	Far cloudy	Pod clear	Far clear	N	
Threshold Accuracy					> 0.85	< 0.20			
Target Accuracy					> 0.90	< 0.15			
Optimal Accuracy					> 0.95	< 0.10			

The target accuracy is reached for the global GAC data validation for all conditions. For twilight the POD(cloudy) is just below or at the target accuracy (if rounding to two decimals it is 0.9 as required), and for daytime the accuracy is actually reaching optimal!

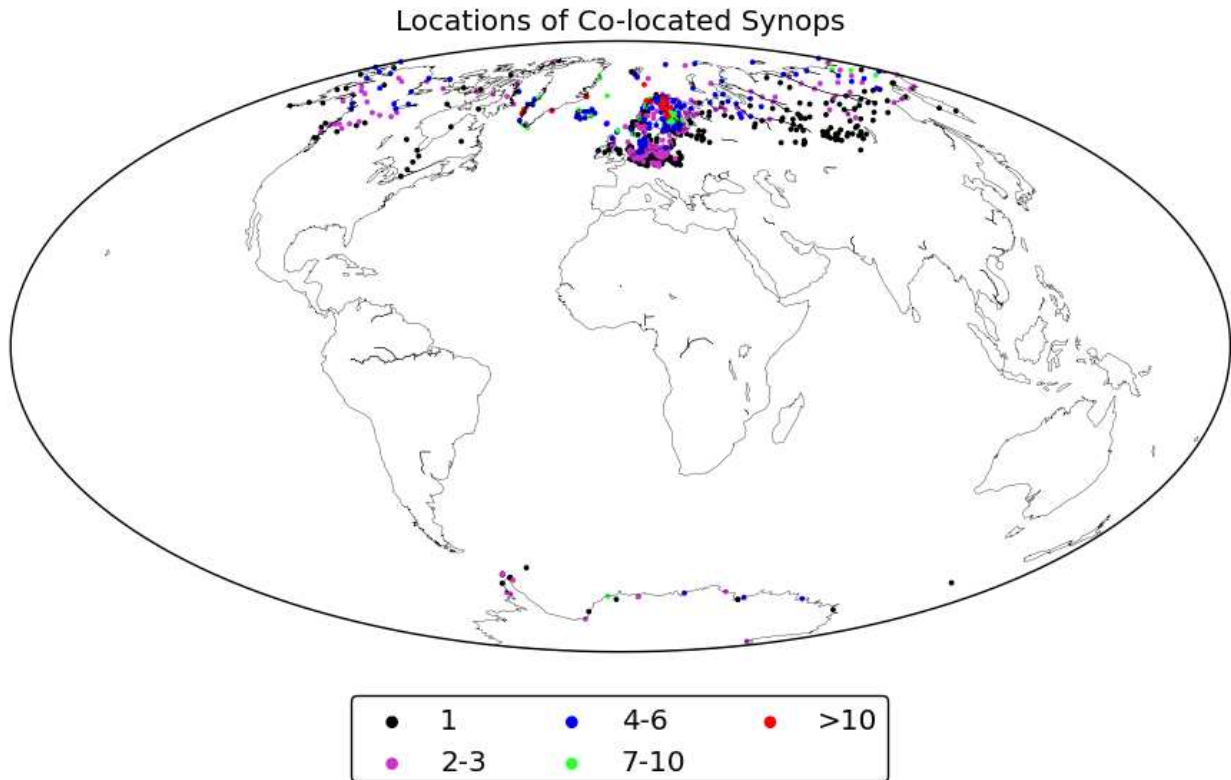


Figure 7: Geographical distribution of Synop/AVHRR GAC collocations in twilight conditions (sun zenith angles between 80 and 95 degrees.)



Figure 8: A quicklook of the USGS landuse over the SMHI production area 'euron1', which we have used here to filter the Synop collocations according to geographical location.

We have reduced this global validation dataset to cover only the European area, by selecting all collocations inside the area shown in Figure 8. This area is one of the bigger areas used in the SMHI operational production. It is positioned so that it contains a little more area west and north of the receiving station in Norrköping as much of the large scale weather originates from west and north-west. The collocations corresponding to that filtering is seen in Figure 9 and the results are displayed in Table 4.

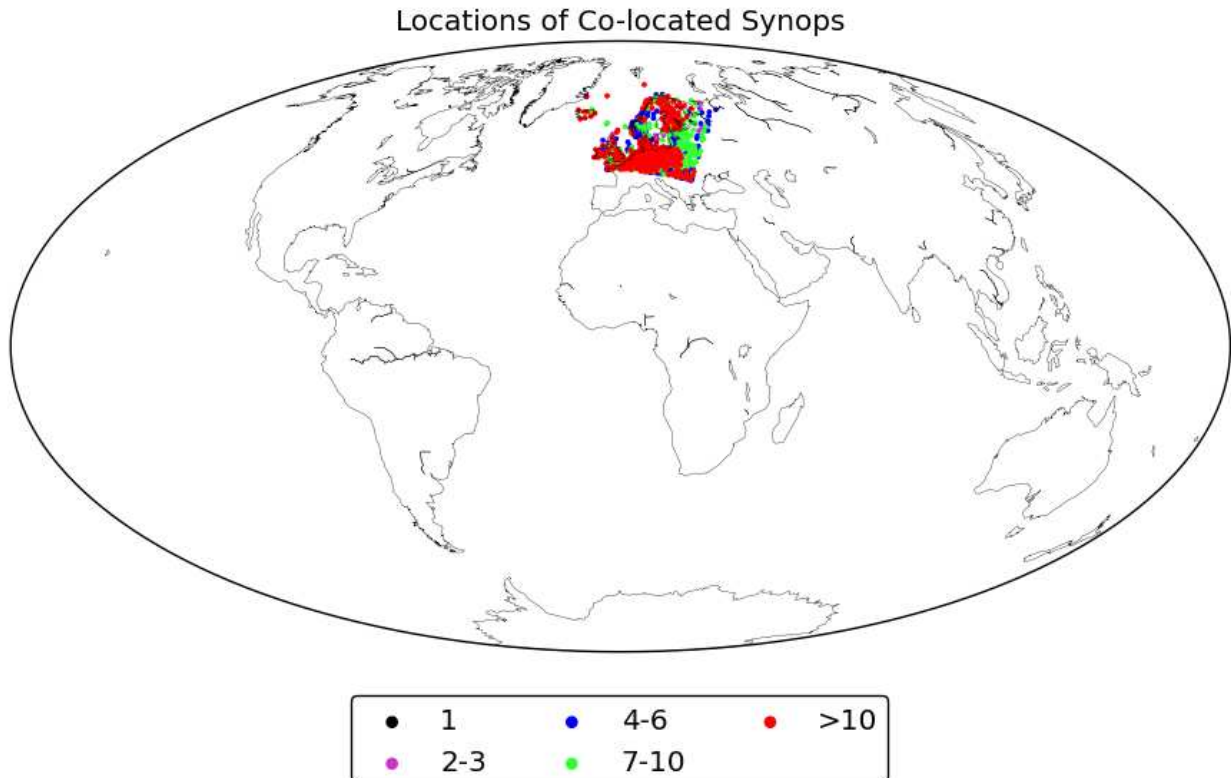


Figure 9: All Synop/AVHRR GAC collocations within in the area defined by 'euron1' (see Figure 8) corresponding to Northern Europe and adjacent Seas.

The results show that the PPS cloud mask v2014 meets the target accuracy on average and during day, but that it only meets the threshold accuracy at night and twilight. However also at night and twilight the cloud mask is well above the target accuracy. Again, like for the global validation the FAR is well below the target accuracy and actually meets the requirements for optimal accuracy except at night.

The corresponding validation using direct readout data from Suomi NPP and NOAA-18 and 19 against Synop reports show a similar, though a slightly worse picture. The threshold accuracy is met in all conditions and the optimal accuracy is met during daytime. Also according to the FAR for cloudy the target accuracy is met in all conditions and the optimal accuracy is met in daytime.

The slightly degraded validation results using DR data compared to GAC data filtered over the European area given by Figure 8 is thought at least partly to be a consequence of the higher amount of Synop reports at high latitudes and in more extreme environments (Greenland and Svalbard and Siberia). See the distribution of collocations in Figure 2. Also the datasets are fairly small so the lack of statistical significance can play a role.

Table 4: Validation scores for 99 GAC orbits against only the Synop reports within the northern European domain, defined by the SMHI production area “*euron1*”. See Figure 8 and Figure 9.

Observed Accuracy									
	RMS	MAE	Hit rate	Bias (%)	Pod cloudy	Far cloudy	Pod clear	Far clear	N
All	2.00	1.27	0.930	0.55	0.956	0.039	0.783	0.238	8994
Day	1.77	1.13	0.950	1.33	0.972	0.029	0.805	0.186	5852
Night	2.38	1.52	0.889	-0.23	0.924	0.064	0.751	0.286	2167
Twilight	2.38	1.56	0.901	-2.45	0.927	0.047	0.766	0.331	975
Target Accuracy (Europe)									
	MAE	Hit rate	Bias (%)	Pod cloudy	Far cloudy	Pod clear	Far clear	N	
Threshold Accuracy					> 0.85	< 0.20			
Target Accuracy					> 0.95	< 0.10			
Optimal Accuracy					> 0.98	< 0.05			

Table 5: Validation scores for the collocations of global Synop reports with the intermittent 2-year dataset of PPS cloudmask on AVHRR and VIIRS from locally received Suomi NPP, NOAA-18 and NOAA-19 data.

Observed Accuracy									
	RMS	MAE	Hit rate	Bias (%)	Pod cloudy	Far cloudy	Pod clear	Far clear	N
All	2.36	1.67	0.904	-6.86	0.927	0.051	0.821	0.241	43182
Day	2.03	1.46	0.939	-6.60	0.953	0.029	0.877	0.189	22898
Night	2.69	1.91	0.868	-6.72	0.905	0.082	0.763	0.268	16309
Twilight	2.77	1.99	0.850	-8.98	0.860	0.065	0.820	0.338	3975
Target Accuracy (Europe)									
		MAE	Hit rate	Bias (%)	Pod cloudy	Far cloudy	Pod clear	Far clear	N
Threshold Accuracy					> 0.85	< 0.20			
Target Accuracy					> 0.95	< 0.10			
Optimal Accuracy					> 0.98	< 0.05			

4.1.2 Caliop validation

It must be stated that accuracy requirements are defined for comparison against European SYNOP stations. In **Table 6** accuracy measures for the cloudmask for locally received data as compared to CALIOP are presented. For the FAR-cloudy target accuracy is reached for all cases. The locally received data includes Europe and Arctic pixels and POD-cloudy is a bit below threshold accuracy; if we consider only the pixels over Europe POD-cloudy is just under the threshold accuracy of 85%. POD-cloudy threshold accuracy is also reached during day and for the filtered case, where clouds with optical thickness below 0.2 are not included. Considering that results for filtering with a detection limit of optical thickness 0.2 hints that around 3% of the clouds are not detected because they are too thin to be detectable by the passive IR/VIS sensors AVHRR and VIIRS. These thin clouds could have been considered clear, but among them are, apart from thin clouds, also clouds which are geographically small. Because the optical thickness is only presented in 5km resolution we choose to not include them at all in this filtered scenario.. For locally received data we can see that we have slightly more matches for version 2012. This is due to different handling of buggy S-NPP granules. Sometimes the first granule received has default time information of the year 1958, and often also such first granules have many missing lines. In PPS version 2014 these problematic

granules are not included in the products. Both POD-clear and POD-cloudy are increased by about 3% in PPSv2014 compared to PPSv2012.

Table 6 Accuracy measures and verification scores for the PPS cloud mask (version 2014) for locally received S-NPP and NOAA-18/19 data over Europe and Arctic as compared to CALIPSO. CALIPSO data for the filtered case are filtered so that pixels with total optical thickness below 0.2 (in the 5km data set, this information is not available in the 1km data set) are not considered. Shown are the observed accuracies, total and also divided by illumination conditions, as well as the required accuracies. HR denotes the hit rate and N the number of matching pixels. Green: within target accuracy. Red: not reaching threshold accuracy.

Observed Accuracy --- Locally received data over Europe							
	BIAS %	HR	POD-cloudy%	FAR-cloudy %	POD-clear %	FAR-clear %	N
PPS 2012 (all)	-12.0	0.81	79.0	5.7	86.4	40.9	796488
PPS (all) unfiltered	-10.2	0.84	82.4	4.5	88.9	36.4	775299
PPS (all) only Europe	-7.2	0.86	86.3	5.0	86.3	38.2	426346
PPS (all) filtered 0.2	-10.2	0.84	82.4	4.5	88.9	36.4	775299
PPS day unfiltered	-5.5	0.87	88.0	5.1	85.6	30.1	296104
PPS night unfiltered	-12.3	0.83	79.5	4.0	91.5	36.3	336888
PPS twilight unfiltered	-15.2	0.80	77.2	4.0	88.6	47.4	142307
Requirement Accuracy (Europe)							
Threshold POD cloudy	Target POD			Optimal POD			
85%	95%			98%			
Threshold FAR cloudy	Target FAR			Optimal FAR			
20%	10%			5%			

Table 7 Accuracy measures and verification scores for the PPS cloud mask (version 2014) for AVHRR-GAC data as compared to CALIPSO. Calipso data for the filtered case are here filtered so that pixels with total optical thickness below 0.2 are considered clear. As a reference the same data set from CLARA-A1 (PPS v2010) is included. Shown are the observed accuracies, total and

also divided by illumination conditions, as well as the required accuracies for SYNOP matches. HR denotes the hit rate and N the number of matching pixels. Green: within target accuracy. Light green: also within target accuracy. Red: not reaching threshold accuracy.

Observed Accuracy --- AVHRR GAC Global data							
	BIAS %	HR	POD-cloudy %	FAR-cloudy %	POD-clear %	FAR-clear %	N
PPS GAC (all) CLARA-A1	-14.2	0.76	73.4	8.4	82.3	45.9	725900
PPS GAC (all)	-11.5	0.77	75.0	9.9	82.3	39.7	785043
PPS GAC (all) filtered 0.2	2.2	0.82	85.5	17.8	77.7	18.4	785043
PPS GAC day unfiltered	-5.9	0.81	80.9	11.2	80.3	31.5	354418
PPS GAC night unfiltered	-15.2	0.75	71.1	9.1	83.8	44.0	362043
PPS GAC twilight unfiltered	-21.3	0.72	67.1	6.4	86.2	53.5	68582
Requirement Accuracy (global)							
Threshold POD cloudy	Target POD			Optimal POD			
85%	90%			95%			
Threshold FAR cloudy	Target FAR			Optimal FAR			
20%	15%			10%			

For the GAC results *Table 7* we see the same general behaviour as for locally received data. We see an improvement compared to CLARA-A1 (pps 2010), specially regarding POD-clear which now reach threshold accuracy for all illumination cases. The improved Hitrate also show that v2014 is better at separating cloudy from clear pixels. The filtered cases for GAC data show decreased POD-clear, this is because pixels with optical-thickness below 0.2 are here considered clear, not excluded. Considering the results for filtering with the detection limit of optical thickness 0.2, it shows that around 8% of the clouds are not detected because they are too thin for the instruments AVHRR and VIIRS to see. The increased number of matching-points is due to that PPS no longer give as much nodata values. It is worth to notice that results are generally improving despite that these more difficult areas now are included. Nodata-values were most common in high terrain, in the arctic, during winter.

At first sight the high values for FAR-clear seems alarmingly high both for locally received data and for the global GAC data. However this measure is very much dependent on the mean cloud fraction cover (mCFC). For this validation data mCFC is 75%. This means that 75% of the pixels considered are cloudy. FAR-clear can be calculated directly from POD-clear, POD-cloudy and mCFC. Even if

we had a POD-clear of 100% we would need a POD-cloudy higher than 96% to reach target accuracy for FAR-clear because of the high mCFC.

4.2 CLOUD TYPE

For a validation of the cloud type, we use the classification provided in the CALIPSO data (at 30 m vertical resolution). CALIPSO cloud types can be condensed into three height classes, which are low- (pressure > 680 hPa), medium- (pressure 440-680 hPa) and high-level (pressure < 440 hPa) clouds. These levels correspond more or less (not exactly because of slightly differing bins) to the PPS cloud classes: Low level clouds, medium level clouds and high + very high level clouds.

Table 8: Relative and absolute fraction of different cloud-classes (distinguished here by cloud height). Presented are results for locally received data over Europe and Arctic and AVHRR GAC data. The comparisons are not straightforward, because only PPS has the class ‘fractional clouds’. From this class, the majority of fractional clouds are in fact low-level fractional clouds. ‘Relative’ refers to ‘fraction of detected clouds’ and ‘absolute’ to ‘fraction of all pixels’.

	Relative Fraction Low %	Relative Fraction Medium %	Relative Fraction High %	Relative Fraction Frac- tional %	Absol. Fraction Low %	Absol. Fraction Medium %	Absol. Fraction High %	Absol. Fraction Frac- tional %
CALIOP (all) 5km	27.0	14.0	59.0	-	18.5	9.6	40.3	-
PPS (all) <u>GAC</u>	27.0	20.4	47.2	5.4	15.4	11.6	26.8	3.1
CALIOP (all)	37.1	22.0	40.8	-	27.6	16.4	30.3	-
PPS (all)	25.2	21.2	45.3	8.3	16.1	13.6	29.0	5.3
CALIOP (day)	43.5	25.1	31.4	-	32.9	18.9	23.7	-
PPS (day)	26.7	22.1	37.7	13.5	18.7	15.5	26.3	9.5
CALIOP (night)	32.2	17.3	51.1	-	22.7	12.4	36.6	-
PPS (night)	25.0	20.1	52.5	2.4	14.8	11.9	31.2	1.4
CALIOP (twilight)	34.7	25.8	39.4	-	27.0	20.1	30.7	-
PPS (twilight)	22.2	21.4	46.6	9.8	13.9	13.4	29.1	6.1

Table 9: Basic accuracy descriptors for the cloud classes: low, medium and high. The ‘bc RMS’ denotes the bias corrected RMS and HR the hit rate. Green: within target accuracy Red: not

reaching threshold accuracy. Presented are results for locally received data over Europe and Arctic and for AVHRR GAC data.

Observed Accuracy					
	Bias %	bc RMS%	POD %	FAR %	HR
<u>GAC</u>					
All: Low	-2.1	42.0	61.9	48.7	0.89
Medium	2.0	49.0	38.0	74.7	0.84
High	-13.5	29.0	65.4	21.8	0.85
<u>Local reception</u>					
All: Low	-11.4	45.6	53.5	26.5	0.86
Medium	-2.8	43.7	38.1	61.5	0.79
High	-1.3	46.4	69.4	39.1	0.82
Day: Low	-14.2	46.3	51.1	22.7	0.83
Medium	-3.4	43.9	41.1	54.0	0.75
High	2.6	45.2	68.0	45.0	0.83
Night: Low	-7.9	44.5	58.4	31.3	0.89
Medium	-0.44	42.3	35.8	70.8	0.82
High	-5.4	46.3	71.2	32.2	0.82
Twilight: Low	-13.1	46.8	50.4	25.0	0.87
Medium	-6.8	46.1	34.9	58.7	0.82
High	-1.5	49.1	66.8	45.4	0.80
Required Accuracy					
	Threshold	Target	Optimal		
POD	50%	70%	80%		
FAR	60%	40%	20%		

In Table 8 and Table 9 the overall performance of the PPS algorithm in sorting detected clouds into classes can be seen; as well for all available cases, as sorted after day/night/twilight. Considering the

<i>EUMETSAT Satellite Application Facility to NoWCASTing & Very Short Range Forecasting</i>	Scientific and Validation Report for the Cloud Product Processors of the NWC/PPS	Code: NWC/CDOP2/PPS/SMHI/SCI/VR/Cloud Issue: 1.0 Date: 15 September 2014 File: NWC-CDOP2-PPS-SMHI-SCI-VR-Cloud_v1_0 Page: 33/67
---	--	---

fractional clouds class is missing from CALIOP, and inspection of these clouds suggests they are mainly low-level, quantitative comparisons indicate a clear agreement between the two satellites. Also for day and night cases, PPS and CALIOP have about the same proportion of clouds in the different classes; only for twilight are there larger differences.

The good agreement appears also in the case of POD, a more demanding criterion. Here, the threshold requirements are also met for low- and high-level clouds, but the detection rate of medium-level clouds misses threshold requirements. For daytime and night and twilight, the pattern is the same as for the average – meeting threshold requirements for low- and high-level clouds, but not for medium-level clouds. We can also see that for some high clouds target accuracy POD is reached or almost reached in all situations.

Threshold requirements for FAR are missed for most medium-level clouds. One needs to bear in mind that evaluation was originally planned against interactive targets, not CALIOP data. High-level clouds just reach threshold requirements for FAR for all cases, and for night it even reaches targeted accuracy. For low-level clouds in all conditions, target performance is met, in terms of FAR. The results are somewhat worse than it was for the AVHRR 2012 comparisons ([RD.2.]), but the degree of reaching threshold and target accuracy is about the same now as it was for v2012.

4.3 CLOUD TOP HEIGHT

In this section, the performance of the cloud top height algorithm is investigated. **Table 10** presents and overview on the general quality for the height determination at several vertical levels and illumination conditions while **Table 11** and **Table 13** focuses on the special requirements. In **Table 12** results are presented for the retrieval rate, the part of clouds detected by the PPS cloudmask that are assigned a height and in **Figure 11** there is visual example of the high retrieval rate of pps v2014. **Figure 10** shows an illustration of CALIOP cloud height compared to PPS cloud height for one swath. The difference between the filtered and the unfiltered data are also visualized in **Figure 10**.

Table 10: A basic description for the comparison of the PPS cloud top height and that, derived by CALIOP. Data considered is locally received data over Europe and Arctic. Given are total results as well as results separated in day/night/twilight. In the filtered data: as cloud top of CALIOP is used the height at 1.0 optical depth down in the cloud.

Comparison to 1km data filtered with 5km CALIOP data	Bias Low (m)	Bias Medium (m)	Bias High (m)	bc-RMS (RMS) Low (m)	bc-RMS (RMS) Medium (m)	bc-RMS (RMS) High (m)	N
All Clouds (filtered)	755	346	-1170	1169 (1408)	1332 (1364)	2365 (2632)	465369
Day (filtered)	834	394	-1325	1271 (1529)	1245 (1297)	2212 (2575)	192987
Night (filtered)	688	270	-1126	1030 (1258)	1449 (1444)	2518 (2752)	188606
Twilight (filtered)	665	354	-1015	1115 (1325)	1333 (1376)	2150 (2336)	83776
Comparison to 1km CALIOP data.	Bias Low (m)	Bias Medium (m)	Bias High (m)	RMS Low (m)	RMS Medium (m)	RMS High (m)	N
All Clouds	515	-343	-2936	1155 (1265)	1357 (1400)	2124 (3624)	473122
Day	640	-101	-2466	1260 (1414)	1253 (1258)	2096 (3237)	192909
Night	386	-667	-3263	1004 (1076)	1434 (1582)	2161 (3914)	197708
Twilight	414	-365	-2769	1160 (1083)	1339 (1388)	1877 (3345)	82505

<i>EUMETSAT Satellite Application Facility to NoWCasting & Very Short Range Forecasting</i>	Scientific and Validation Report for the Cloud Product Processors of the NWC/PPS	Code: NWC/CDOP2/PPS/SMHI/SCI/VR/Cloud Issue: 1.0 Date: 15 September 2014 File: NWC-CDOP2-PPS-SMHI-SCI-VR-Cloud_v1_0 Page: 35/67
---	--	---

For the filtered data results are quite similar for all illumination conditions. As expected the mean (Bias) is increased with the filtering, because we generally compare with lower cloud tops. For high clouds the filtering increases bc-RMS a little. For the unfiltered data there are more differences in Bias between different illumination conditions, this difference can be due to that there are more optically thin geometrically thick high- and medium-level clouds during night in this data set. For the threshold, target and optimal accuracies as defined in the PRD ([AD.4.]), .

Table 11: Observed and required accuracies for the cloud top heights for locally received data over Europe and Arctic. Green: within target accuracy. Light green: also within target accuracy. Red: not within threshold accuracy. For the semi-transparent and opaque clouds together the bias is: -1100m, the RMS is 2535m and bc-RMS 2284m (unfiltered CALIOP data).

		Observed Accuracy							
		Semi-transparent				Opaque			
		All	Low	Medium	High	All	Low	Medium	High
<u>Filtered cloud top</u> Very thin top layer	Bias	203	1545	947	-1405	-948	630	-214	-2829
	RMS	2498	2267	1894	2980	2745	1195	1526	4043
	bc-RMS	2487	1658	1640	2628	2576	1015	1511	2888
<u>Filtered cloud top</u> Thicker clouds	Bias	148	951	724	-426	-186	424	-127	-1313
	RMS	1739	1532	1242	1977	1445	870	943	2294
	bc-RMS	1732	1201	1009	1931	1433	760	934	1881
<u>Unfiltered</u> All clouds	Bias	-976	944	153	-2579	-1226	227	-909	-3533
	RMS	2525	1723	1253	3247	2545	854	1579	4174
	bc-RMS	2329	1441	1245	1969	2231	823	1292	2223
<u>Unfiltered All clouds</u> PPS v2012	Bias	-561	1167	418	-2573	-1309	478	-839	-3566
	RMS	2441	1793	1275	3313	2717	951	1453	4190
	bc-RMS	2375	1361	1204	2087	2380	822	1186	2200
		Semi-transparent			Opaque				
		Threshold	Target	Optimal	Threshold	Target	Optimal		
Bias	2000 m	1500 m	200 m	1000 m	500 m	200 m			
bc-RMS	2000 m	1500 m	500 m	2000 m	1500 m	500 m			

The results in **Table 11** should be taken as an approximate estimate, i.e. results so far are in the right magnitude. As mentioned before, the restrictions due to the sensor differences are also valid for the

<i>EUMETSAT Satellite Application Facility to NoWCASTing & Very Short Range Forecasting</i>	Scientific and Validation Report for the Cloud Product Processors of the NWC/PPS	Code: NWC/CDOP2/PPS/SMHI/SCI/VR/Cloud Issue: 1.0 Date: 15 September 2014 File: NWC-CDOP2-PPS-SMHI-SCI-VR-Cloud_v1_0 Page: 37/67
---	--	---

cloud height inter-comparison. However, the CALIPSO database comes closest to what a trustworthy and continuous dataset should look like but more efforts to assure a fair comparison need to be taken. The filtered data provides a more fair method for comparison than the unfiltered data. The limit (optical thickness 1.0) and the method is not perfect, for example the optical thickness information is only present in the 5km data and how this is best used for 1km data can be investigated further. However the filtered data results support the theory that the much larger Bias and RMS-error for high clouds is mainly caused by sensor differences.

Table 11 shows cloud top height results for locally received AVHRR/VIIRS data over Europe and Arctic. The CTHH product, both for semi-transparent and for opaque clouds, reaches the threshold and often also the target accuracy in terms of bias and bc-RMS for medium-level and low-level clouds. For high-level clouds of the unfiltered data the threshold accuracy is reached only for bc-RMS semi-transparent; especially the Bias is far from threshold accuracy. One reason for this is the sensor differences discussed. In the results for the filtered data, split in two categories, we can see (as in **Table 10**) that the Bias and RMS are much closer to target accuracies. This is because in the filtered data we compare the PPS cloud top to a more fair cloud top of CALIOP. The filtered results are much more close to threshold accuracy for high clouds. For all the semi-transparent and opaque clouds together the bias is: -119 m, and the RMS is 2003m and the bc-RMS is 1999m (filtered CALIOP data). The due to compensation of systematic errors of high and low clouds, the bias is within optimal accuracy. The bc-RMS is just within threshold accuracy.

Also by separately considering the cases where the top-layer in CALIOP is too thin for AVHRR/VIIRS to detect at all (optical thickness below AVHRR detection limit 0.2 see Karlsson and Johansson 2013) we can see that the largest problems occur when we have a very thin top cloud layer. For these cases we don't expect CALIOP and AVHRR to be able to detect the same height. For the data where we do expect AVHRR/VIIRS and CALIOP to detect the same cloud top (Thicker clouds) and where we compare to a fair CALIOP cloud top (Filtered cloud top) all measures are within threshold accuracy except the bias (-1292m) for high opaque clouds; the bias for high opaque clouds is not too far from the threshold accuracy. For the filtered thicker clouds the combined bias is -15m (within optimal threshold, but due to compensating errors for high and low clouds) and bc-RMS is equal to the RMS which is 1604m which are within threshold accuracy and near target accuracy.

The problem with the high bias observed for opaque high-level clouds can also be because some high-level clouds are still treated with the opaque algorithm, when they in fact exhibit a certain semi-transparency which is not corrected for, or even worse assigned an "opaque" cloud type to multilevel clouds which is not detected properly in PPS for most cases. These effects are demonstrated in a visiting scientist report [RD.4.]. In version PPS v2014 there are some efforts made to decrease this problem and some opaque clouds suspected to be semi-transparent are now treated with the semi-transparent algorithm.

Compared to version 2012 we can see that the Bias is improving 200m for low clouds for both algorithms and also 200m for medium-level semi-transparent clouds. Other changes are small around or below 100m. Notice that it is no the exact same data sets that are compared between the version because a lot of the semi-transparent clouds present in the version 2014 dataset, where only getting

no-data height in PPS version 2012. The retrieval rate for CTTH is increased a lot with version 2014 (see **Table 12**). Remember also that PPS v2014 CMA and there for also CTTH also have data over Greenland during polar winter. So generally stats are about the same or slightly better at the same time as more difficult clouds are included.

Table 12 Retrieval rate for PGE03 for PPS version 2014 compare to version PPS v 2012 or v2010.

Data set	Retrieval Rate	
	PPS v2014	PPS v2010/v2012
GAC Global data	97.0%	66.3%
Suomi-NPP Europe and Arctic	98.4%	72.1%
Noaa18/19 Europe and Arctic	98.5%	78.9%

Table 13 Observed and required accuracies for the cloud top heights for AVHRR GAC data.
Green: within threshold accuracy. Light green: also within target accuracy. Red: not within threshold accuracy. Semi-transparent and opaque results are presented together. Included are for comparison results for the same orbits from CLARA-A1 (PPS v2010).

Observed Accuracy GAC-data								
	Bias				bc-RMS/ (RMS)			
	All	Low	Medium	High	All	Low	Medium	High
<u>GAC CLARA-A1</u>	-2714	602	-763	-5256	3963	1147	1503	3735
Retrieval rate: 66.3%					(4803)	(1295)	(1686)	(6448)
<u>GAC PPS v2014</u>	-1995	739	-175	-3722	3500	1607	1703	3428
Retrieval rate: 97.7%					(4028)	(1769)	(1712)	(5060)
Required Accuracy								
	Semi-transparent			Opaque				
	Threshold	Target	Optimal	Threshold	Target	Optimal		
Bias	2000 m	1500 m	200 m	1000 m	500 m	200 m		
bc-RMS	2000 m	1500 m	500 m	2000 m	1500 m	500 m		

For the cloud top height for GAC we can see that the total results are improved compared to PPS v2010 used for CLARA-A1. The total Bias is improved with 300m and the total bc-RMS with 400m. The Bias improvement is around 1km for high-level clouds and a few hundred meters for low- and medium level clouds. For high-level clouds bc-RMS is improved with 100m and for medium- and low-level clouds bc-RMS is 100-200m worse. The reason for this is probably the increased retrieval rate. The retrieval rate is much improved for GAC data (**Table 12**). The retrieval rate is the part of the detected clouds (pixel cloudy both according to PPS and CALIOP) that have been assigned a height. Much of these clouds are semi-transparent and the reason they now get a height is the improvements of the semi-transparent algorithm in PPS v2014. The reason that bc-RMS for low-level and medium-level clouds is a bit worse than before is probably because the opaque algorithm performs much better than the semi-transparent algorithm for lower clouds together with the fact that a larger part of the lower clouds in the data is now semi-transparent. The improved stats for high clouds is also to a large part because more semi-transparent clouds are now assigned heights. Notice that the scores are in total improving although more of the “difficult” clouds are now included. Remember that for the GAC data the PPS cloud top is compared to the middle of the CALIPSO cloud, this is the same method used for comparisons in other studies of CLARA-A1 (Karlsson, K.-G. and E. Johansson, 2013).

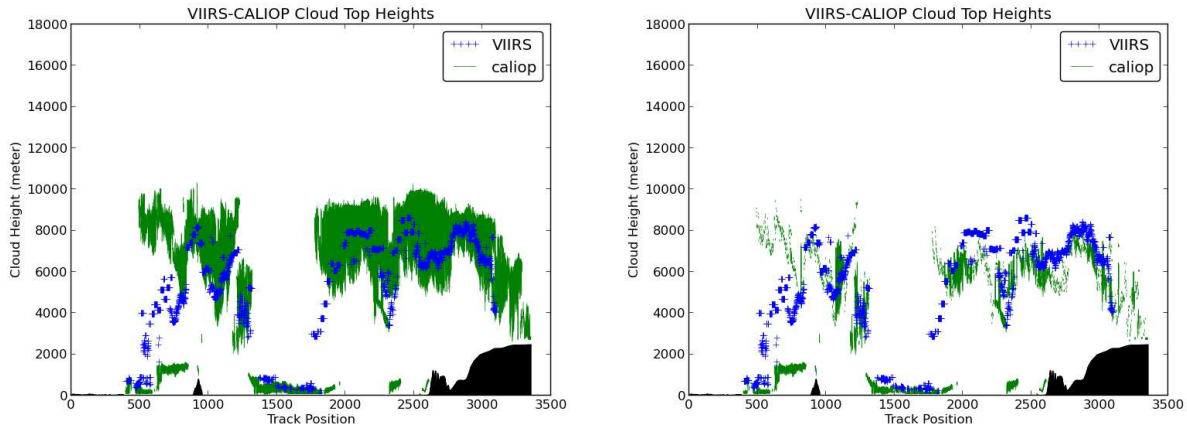


Figure 10 Cloud top heights from CALIPSO (top edge of green area) and PPS on VIIRS (blue) for one swath where PPS performed poorly for unfiltered data (left) and better for filtered data (right). This is due to optically thin clouds in the top layer. PPS is not capturing accurate cloud top height from a multiple cloud layer scene (track position 500-1000). In this swath almost all the high clouds were optically thin (<1.0), and this is why so much of them is removed in the filtering. The low opaque clouds are optically much thicker and the filtering does not remove much of these. The swath is from 2012 October 4:th at around 7:AM, orbit number 4851. And the black land to the right in the picture is Greenland.

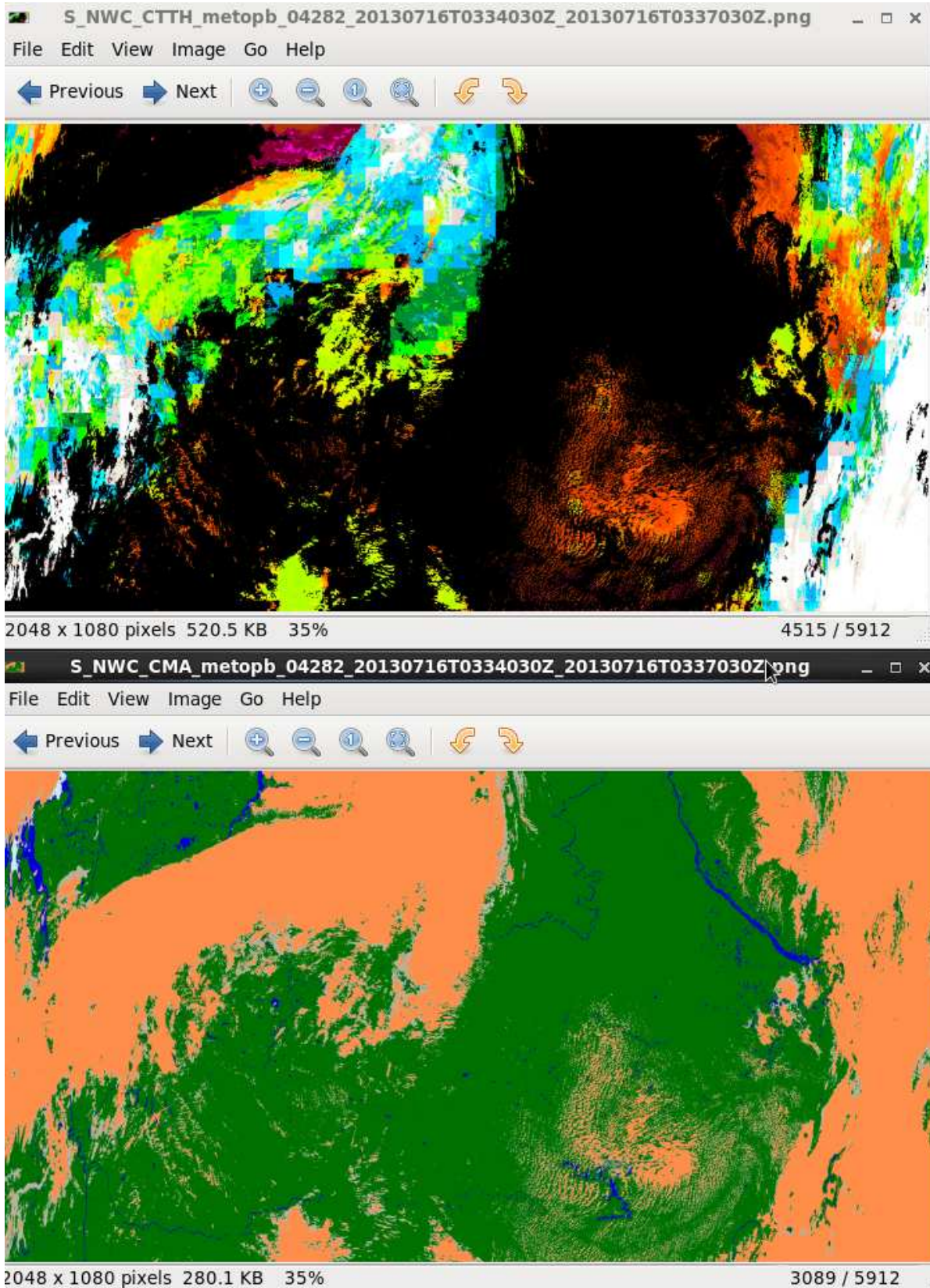


Figure 11 Example of CMA and CTTH of a metop granule, 2013 16:th June, at 03:34. Notice that most clouds in the cloudmask have heights in the CTTH.

4.3.1.1 Study of surface emissivity as input

While making RTTOV simulation, so far we have used default surface emissivity. We made a try to instead use actual surface emissivity as input to the RTTOV simulations. But we decided to stay the old way, using default surface emissivity. Some results are presented in **Table 14**.

Table 14: Cloud top heights for locally received data over Europe and Arctic. Comparing using default and using actual surface emissivity as input to RTTOV. Results are filtered.

		Observed Accuracy							
		Semi-transparent				Opaque			
		All	Low	Medium	High	All	Low	Medium	High
<u>Not using surface emissivity</u>	Bias	177	1228	809	-706	-422	472	-159	-1886
	RMS	2045	1910	1525	2311	1947	955	1194	3074
	bc-RMS	2037	1463	1293	2201	1901	830	1183	2427
<u>Using surface emissivity</u>	Bias	189	1250	818	-700	-391	523	-142	-1875
	RMS	2048	1924	1528	2310	1940	986	1179	3059
	bc-RMS	2039	1463	1291	2201	1900	836	1170	2417
		Semi-transparent				Opaque			
Threshold		Target		Optimal	Threshold	Target		Optimal	
Bias	2000 m	1500 m		200 m	1000 m	500 m		200 m	
bc-RMS	2000 m	1500 m		500 m	2000 m	1500 m		500 m	

Checking the results of the re-validated cloud top heights, it seems that it doesn't give a consistent picture. Both runs (with and without explicit surface emissivity) provide statistical moments superior to that of the other run. Additionally it is noteworthy, that the use of the 'real' emissivity also has consequences on the opaque cloud result. This is certainly because of the newly introduced method to do the atmospheric correction - even for opaque clouds - without cloudy but only with cloudfree simulations.

It is questionable if both methods (atmospheric correction without cloudy simulation and explicit use of emissivity) should be used at the same time. Since both options are configurable, a check that those methods are not combined is suggested. As we already decided to go for atmospheric correction without cloudy simulation in v2014 (as default option), we propose not to use explicit emissivities (as default option). Except for **Table 14**, the validation results presented never use explicit surface emissivity.

<i>EUMETSAT Satellite Application Facility to NoWCASTing & Very Short Range Forecasting</i>	Scientific and Validation Report for the Cloud Product Processors of the NWC/PPS	Code: NWC/CDOP2/PPS/SMHI/SCI/VR/Cloud Issue: 1.0 Date: 15 September 2014 File: NWC-CDOP2-PPS-SMHI-SCI-VR-Cloud_v1_0 Page: 43/67
---	--	---

4.4 CLOUD PHYSICAL PROPERTIES

4.4.1 CPP cloud phase (cph)

Cloud phase, as it is seen from a satellite, is a measure that describes whether the dominant number of observed photons is reflected/emitted by solid or liquid water particles. The penetration depth, the position and size of the probed layer is dependent on the observing wavelength as well as on the cloud composition. This implies that an earthbound observer is likely to probe different volumes, i.e. there is no ground truth for the cloud phase.

The most reliable source for a cloud phase determination from the current A-Train instruments is represented by the active laser probe CALIOP on board the CALIPSO platform. The decision, liquid or ice phase, is made on basis of the depolarization ratio of the backscattered signal (see Hu et al., 2009 for details). A known problem that reduces the quality of the cloud phase product is the detection of multiple scattered radiances. Another problem, that of horizontally oriented ice crystals, has been taken into account by tilting the instrument (to 3° off nadir) and enhancing the viewing zenith angle in 2007 (Hu et al., 2009). One other problem is that if we have a multilayer cloud the different layers can have different cloud phase. This could be a problem if the top layer is too thin for AVHRR to detect. We then compare the cloud phase calculated for PPS on one cloud layer with the CALIPSO cloud phase of a different layer. This is even a problem in case of no physical separation of these layers, i.e. a water cloud with a thin iced top may (for a passive instrument) still reflect/emit the radiative pattern of a water cloud. We tried to tackle this challenge by using only pixels where the upper three CALIOP levels give a concordant phase.

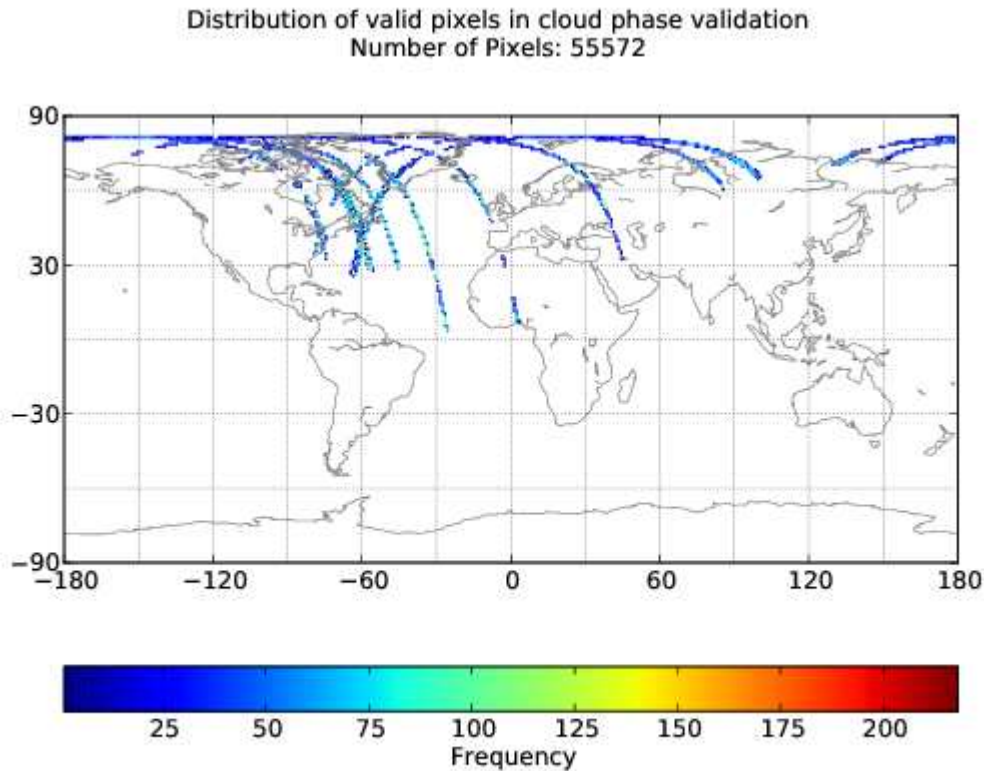


Figure 12: Geographical distribution of measurements considered for this inter-comparison. Valid is the nearest AVHRR pixel within 1km radius to the CALIOP pixel centre if the quality of the CALIOP product is not flagged as poor quality (note that different products have different quality flags. Therefore geographical distribution may vary with cloud product).

From Figure 12 it is easily seen that the distribution is not global or even. All AVHRR data for this validation are acquired from the EUMETSAT Advanced Retransmission Service (EARS). Therefore the covered area is restricted to the domain of direct readout stations. However, Figure 12 shows also that a broad variety of landscapes, surface types and climate regions are taken into account for this study.

The CPP Cloud Phase gives either liquid water or ice, while the CALIOP Cloud Ice/Water Phase Discrimination uses the classes: ice, water and oriented plates. The classes liquid and water are considered as a match. The CPP class ice is considered a match with the two CALIOP classes: ice and oriented plates.

Annual variability:

The data sample for cloud phase validation encompass four months of 2010, namely January, April, July and October, which makes the selection a representative summary, featuring the characteristic annual variations. This is basically the same data set as that, used for the validation of PPS version 2012. But for the version 2012 validation, only daytime results were used (solar zenith angle below 72°). Also, minor deviations may occur due to improvements in the current cloud mask algorithm. Temporal and spatial assignment is displayed in Figure 13.

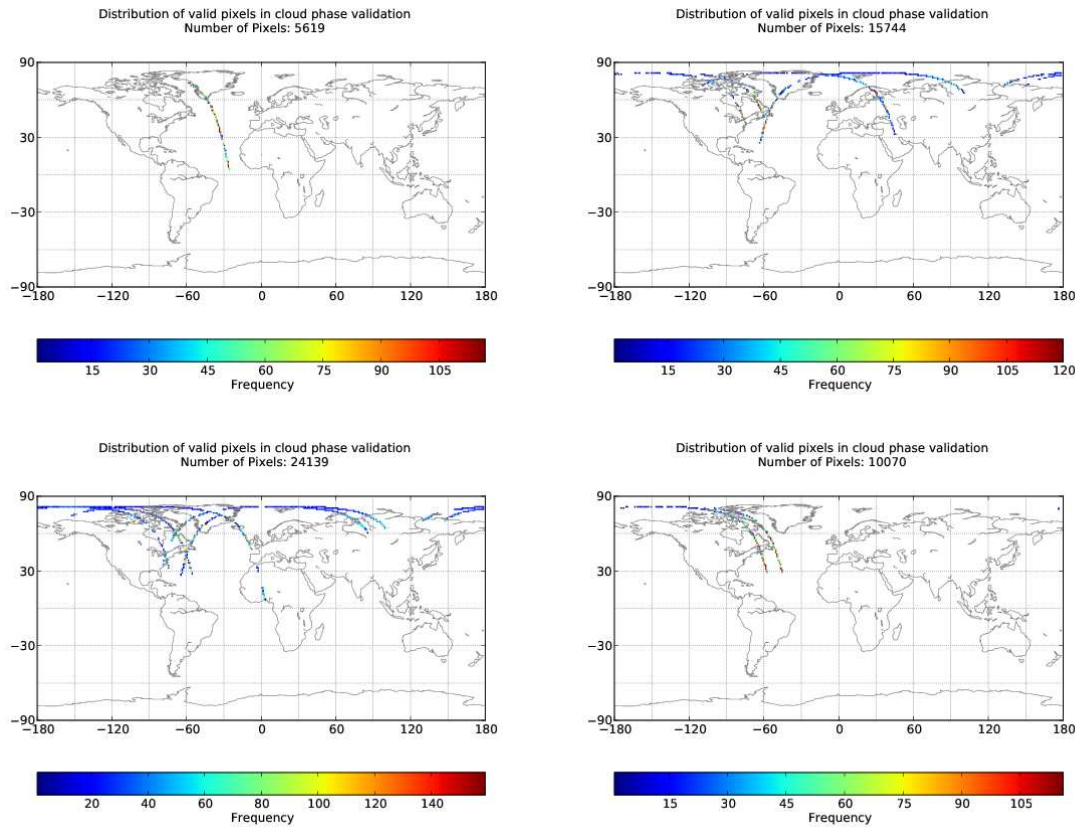


Figure 13: Distribution and location of measurement points for the year under investigation (2010). Upper left January, upper right: April, lower left July and lower right October.

The listing in Table 15 displays seasonal changes in algorithm performance. In Table 16, the corresponding accuracy scores are given. Note that there is a systematic change in distributions of liquid and solid particles (CALIOP results are assumed to represent the truth). In January the majority of pixels are assigned to ice phase clouds. Scenes from April provide a moderate domination of liquid particles while for the July and October cases liquid phase pixels are dominating. These distribution differences do have an effect on the calculated skill scores (POD and FAR) for liquid and solid detection, while the hit-rate (given additionally as an alternative measure in Table 16) remains almost unaffected by these distribution differences.

Note also that this statistic covers day as well as night pixels while the validation of version 2012 was only possible for pixels with daylight conditions.

Table 15: Success matrix for individual months.

		CALIOP liquid	CALIOP solid
January	CPP liquid	782	460

		CALIOP liquid	CALIOP solid
	CPP solid	366	3561
April	CPP liquid	6263	1626
	CPP solid	1991	3841
July	CPP liquid	9521	1767
	CPP solid	3096	7344
October	CPP liquid	3627	617
	CPP solid	2148	2846

Table 16: Success measures for individual months. For version 2014 values are for all solar zenith angles. Numbers in brackets are from the validation of version 2012, which only were during daytime (solar zenith angle below 72°) [RD.3.].

	Hit rate	POD liquid	FAR liquid	POD solid	FAR solid
January	0.84 (0.78)	0.68 (0.81)	0.37 (0.59)	0.89 (0.77)	0.09 (0.05)
April	0.74 (0.73)	0.76 (0.88)	0.21 (0.33)	0.70 (0.56)	0.34 (0.17)
July	0.78 (0.84)	0.75 (0.96)	0.16 (0.17)	0.81 (0.63)	0.30 (0.12)
October	0.70 (0.77)	0.63 (0.87)	0.15 (0.20)	0.82 (0.55)	0.43 (0.31)
All months	0.76 (0.79)	0.73 (0.92)	0.18 (0.23)	0.80 (0.64)	0.30 (0.15)

4.4.1.1 Study of cloud phase and illumination

With version 2014, a new cloud phase algorithm has been introduced. In contrast to its antecessor the new scheme is able to derive a cloud-phase even under night time conditions. To estimate the influence of varying illumination, the complete dataset has been split into one part with daytime condition (in analogy to version 2012 this is true if the solar zenith angle is below 72°) and another part with low level illumination (solar zenith angle above 72°). This study was made with a preliminary version of 2014, but the conclusions should be valid for version 2014 as well. Figure 14 shows the geographical distribution of both these datasets.

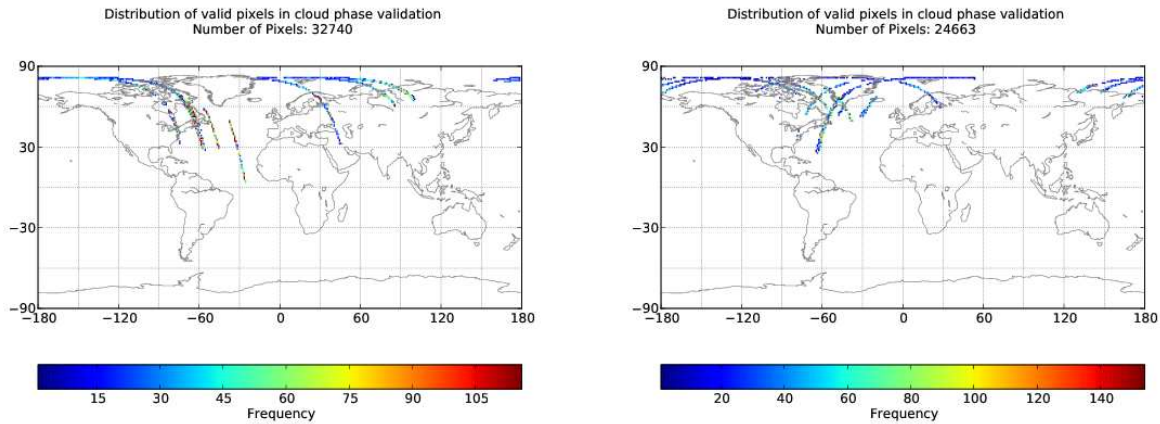


Figure 14: Distribution and location of measurement points separated by illumination conditions. Day (solar zenith angle below 72°) left and night (solar zenith angle above 72°) to the right.

The matrix, showing the frequency of correct and incorrectly classified pixels for this part of the study is shown in **Table 17**. The data sub-set with daytime illumination provides a domination of liquid phase pixel, while the nighttime set show a slight overbalance of pixel with solid cloud phase. The majority of total data was observed during daytime light conditions.

Table 17: Success matrix for day and night.

		CALIOP liquid	CALIOP solid
Day	CPP liquid	12653	2620
	CPP solid	4527	9808
Night	CPP liquid	7471	2659
	CPP solid	3331	8601

Table 18: Success measures for day and night.

	Hit rate	POD liquid	FAR liquid	POD solid	FAR solid
Day	0.76	0.74	0.17	0.79	0.32
Night	0.73	0.69	0.26	0.76	0.28

Comparing the required scores (**Table 20**) with the algorithm performance for Land and sea pixels (**Table 18**) shows that the threshold criteria for all measures within both sub-samples are fulfilled, except for the night time POD liquid. Here the threshold is missed by 0.01. For the liquid FAR the target accuracy is reached, and POD solid almost reaches target accuracy.

<i>EUMETSAT Satellite Application Facility to NoWCasting & Very Short Range Forecasting</i>	Scientific and Validation Report for the Cloud Product Processors of the NWC/PPS	Code: NWC/CDOP2/PPS/SMHI/SCI/VR/Cloud Issue: 1.0 Date: 15 September 2014 File: NWC-CDOP2-PPS-SMHI-SCI-VR-Cloud_v1_0 Page: 48/67
---	--	---

This result proves that the new algorithm is able to derive the cloud phase product under night time conditions. Generally, the performance during daytime is better (except for the solid FAR case). We will recommend the usage of CPP-cloud phase for all lightening conditions, but make it configurable for the user.

4.4.1.2 CPH Performance in total

Studies on sub-samples with focus on different environmental parameters (temporal and spatial) showed that dependencies are not pronounced (except for the new application during night time). Detected variations in the success-measures are rather due to differences in the distribution of solid and liquid particles. The algorithm itself is likely to perform stable.

For the evaluation of the performance of the cloud phase algorithm, results from studies on subsamples are of minor importance. The crucial point is that requirements are met by the entire data base (see *Table 20* for results).

As compared to the phase algorithm in version 2012, performance for detection of liquid phase decreases, while detection performance for solid phase increases. This gives overall a more balanced algorithm performance which still lies within requirements. The new algorithm additionally provides phase retrieval for night time (including twilight) which overall meets or exceeds threshold requirements. Retrievals are now also provided for sunglint areas, which were generally excluded in v2012.

Table 19: Success matrix for the complete data set.

	CALIOP liquid	CALIOP solid
CPP liquid	20193	4470
CPP solid	7601	17592

Table 20: Success measures for complete dataset and according requirements.

	POD liquid	FAR liquid	POD solid	FAR solid
Achieved performance	0.73 (0.92)	0.18 (0.23)	0.80 (0.64)	0.30 (0.15)
Threshold accuracy	≥ 0.70	≤ 0.35	≥ 0.60	≤ 0.35
Target accuracy	≥ 0.80	≤ 0.20	≥ 0.80	≤ 0.20
Optimal accuracy	≥ 0.90	≤ 0.10	≥ 0.90	≤ 0.10

Table 19 shows the matrix of passed and failed phase assignments for the complete validation dataset. The majority of the sample consists of liquid-phase pixels. The overall performance with achieved skill scores and defined requirements is given in **Table 20** (achievements from 2012 version [RD.3.] are given in brackets). The threshold accuracy is met for all scores under investigation. Keeping in mind that the version 2014 dataset comprises even pixel under nighttime illumination conditions, the new algorithm can be seen as an improvement.

Global validation of CPH:

There has also been made a validation of CPP cloud phase, using 99 cases of GAC-data.

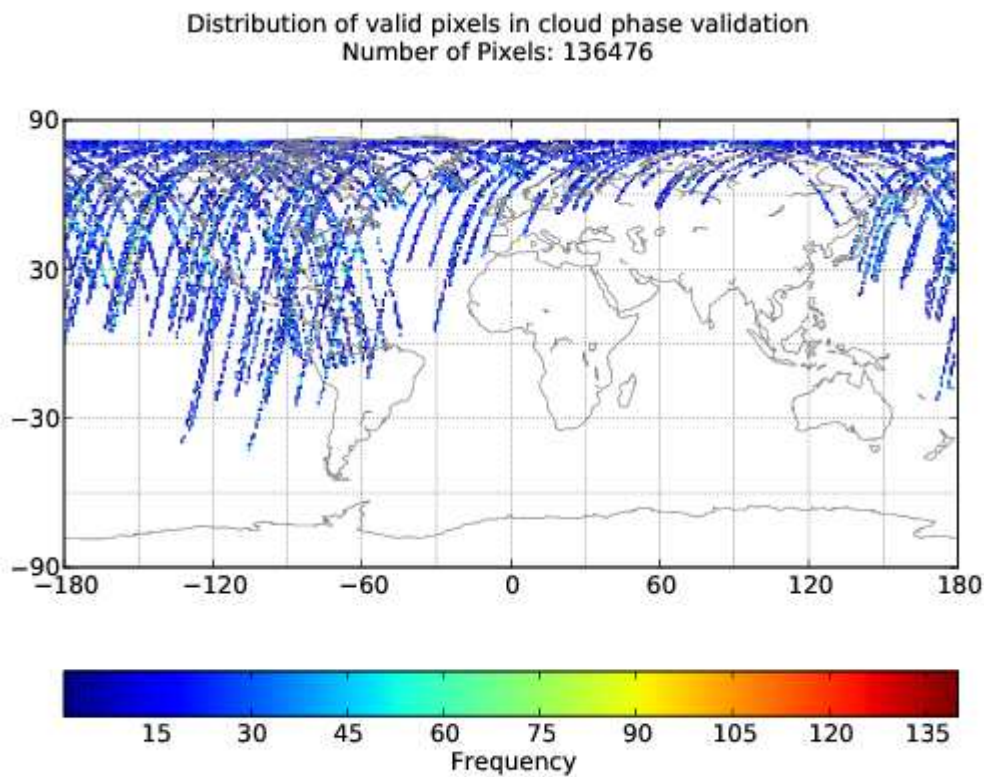


Figure 15 Geographical distribution of the matches between CALIOP pixels and GAC pixels for the CPP cloud phase product).

Table 21: Success matrix for the GAC data set.

	CALIOP liquid	CALIOP solid
CPP liquid	41618	17143

<i>EUMETSAT Satellite Application Facility to NoWCasting & Very Short Range Forecasting</i>	Scientific and Validation Report for the Cloud Product Processors of the NWC/PPS	Code: NWC/CDOP2/PPS/SMHI/SCI/VR/Cloud Issue: 1.0 Date: 15 September 2014 File: NWC-CDOP2-PPS-SMHI-SCI-VR-Cloud_v1_0 Page: 50/67
---	--	---

CPP solid	12600	45982
------------------	-------	-------

Table 22: Success measures for GAC dataset and according requirements.

	POD liquid	FAR liquid	POD solid	FAR solid
Achieved performance	0.77	0.29	0.73	0.22
Threshold accuracy	≥ 0.70	≤ 0.35	≥ 0.60	≤ 0.35
Target accuracy	≥ 0.80	≤ 0.20	≥ 0.80	≤ 0.20
Optimal accuracy	≥ 0.90	≤ 0.10	≥ 0.90	≤ 0.10

The threshold accuracy is received for all measurements.

<i>EUMETSAT Satellite Application Facility to NoWCasting & Very Short Range Forecasting</i>	Scientific and Validation Report for the Cloud Product Processors of the NWC/PPS	Code: NWC/CDOP2/PPS/SMHI/SCI/VR/Cloud Issue: 1.0 Date: 15 September 2014 File: NWC-CDOP2-PPS-SMHI-SCI-VR-Cloud_v1_0 Page: 51/67
---	--	---

4.4.2 CPP liquid water path (lwp)

4.4.2.1 LWP validation within the EARS domain

Up to now, one of the most feasible methods to determine the vertical integrated liquid water content of the atmosphere is the observation of emissions in the microwave spectral range. Over sea we validated the CPP liquid water path retrieval with AMSR-E estimates of LWP.

The most important advantage of microwave LWP retrievals is that it is dependent on fewer assumptions, than is possible for retrievals based on observations in VIS and IR channels. Still, this method is far from being perfect, i.e. Greenwald (2009) identified strong dependencies of the AMSR-E LWP product on surface wind speed but over open water it is still superior to all other methods with comparable temporal and spatial coverage.

To keep the absorption coefficient within the valid range, rain contaminated pixels have to be excluded. Unfortunately, the naturally emitted energy is very low in this wavelength band (typically between 0.9 and 1.3 cm). This requires large antennas, which leads on the other hand to large FOVs and thus a rather rough spatial resolution.

Due to complex contributions from land surfaces, LWP results based on microwave observations are only applicable if the footprint is not 'land-contaminated'.

For this study the LWP product of the Advanced Microwave Scanning Radiometer for EOS (AMSR-E) onboard the AQUA platform is used to provide the reference data. More information on the AMSR-E data set used can be found in section 3.5 and at <http://nsidc.org/data/amsre/>.

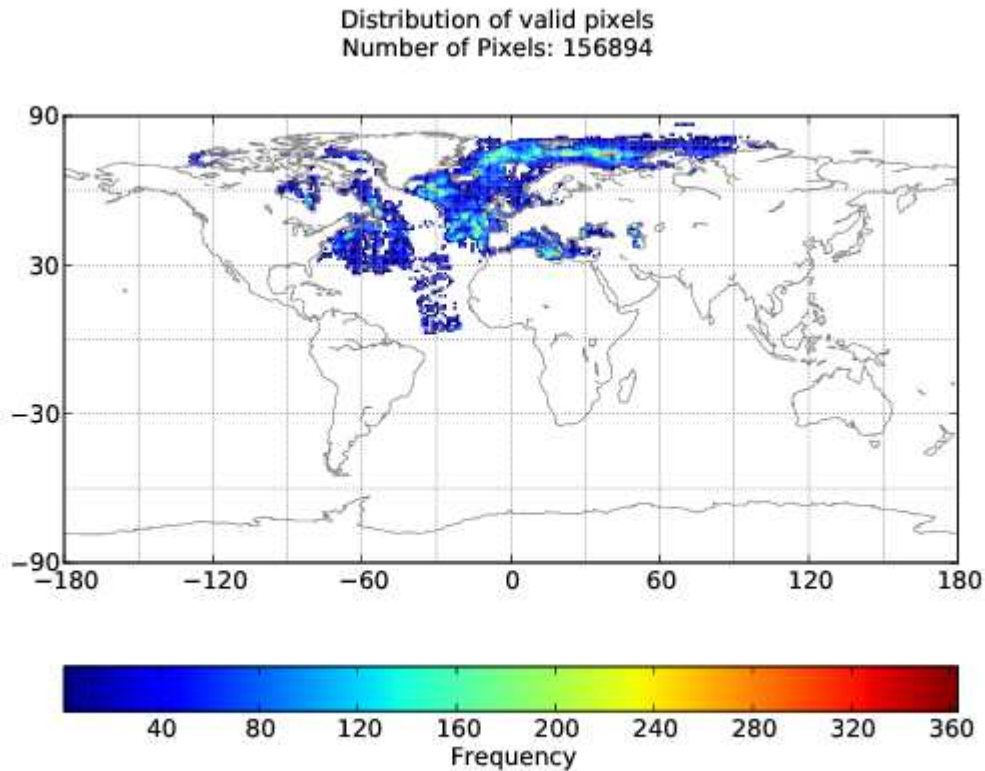


Figure 16: Spatial frequency distribution of used AMSR-E pixel. Matching conditions were extended to: No land pixels, no ice phase in footprint (according to the CPP product), AMSR-E LWP between 0 and 170 g/m² and CPP LWP > 0 g/m².

Just as the for cloud phase, the considered area for inter-comparison of LWP is restricted to the EARS domain (see Figure 16). To avoid contamination by rain, the validation is restricted to a AMSR-E LWP between 0 g/m² and 170 g/m² matched to CPP LWP of greater than 0 g/m², the average of the AVHRR pixels within the AMSR-E footprint is compared to the AMSR-E estimate, which has a resolution of approximately 12km². All time differences are less than 5minutes. Possible parallax effects are not taken into account and can be up to the order of 1 AMSR-E pixel displacement.

Annual variability:

To check seasonal stability, the LWP algorithms performance is displayed separately for available months. Figure 17 shows the spatial distribution of the 4 cases (January, April, July and October) under investigation.

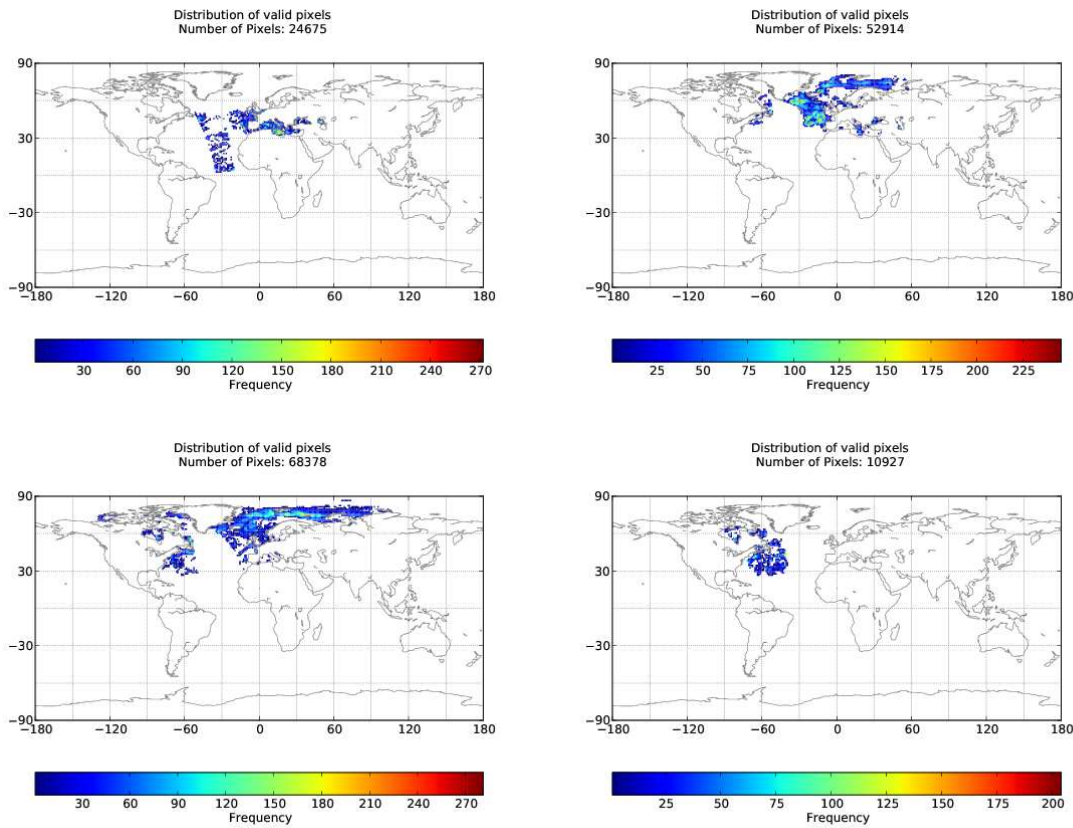


Figure 17: Spatial distribution of observations by month. Upper left: January, upper right: April, lower left: July and lower right October. Note: Solar zenith angle is restricted to 72° (as in previous investigations for version 2012).

Unfortunately, spatial and temporal pattern of the distribution frequency seem to be correlated. The more or less compact cluster for January, April and October do not allow for unambiguous attribution of possible performance variations to either spatial or temporal variations. This might be due to the rather short observation period used. For the study on annual variations only daytime pixels (solar zenith angle below 72°, as it was standard for version 2012) are used.

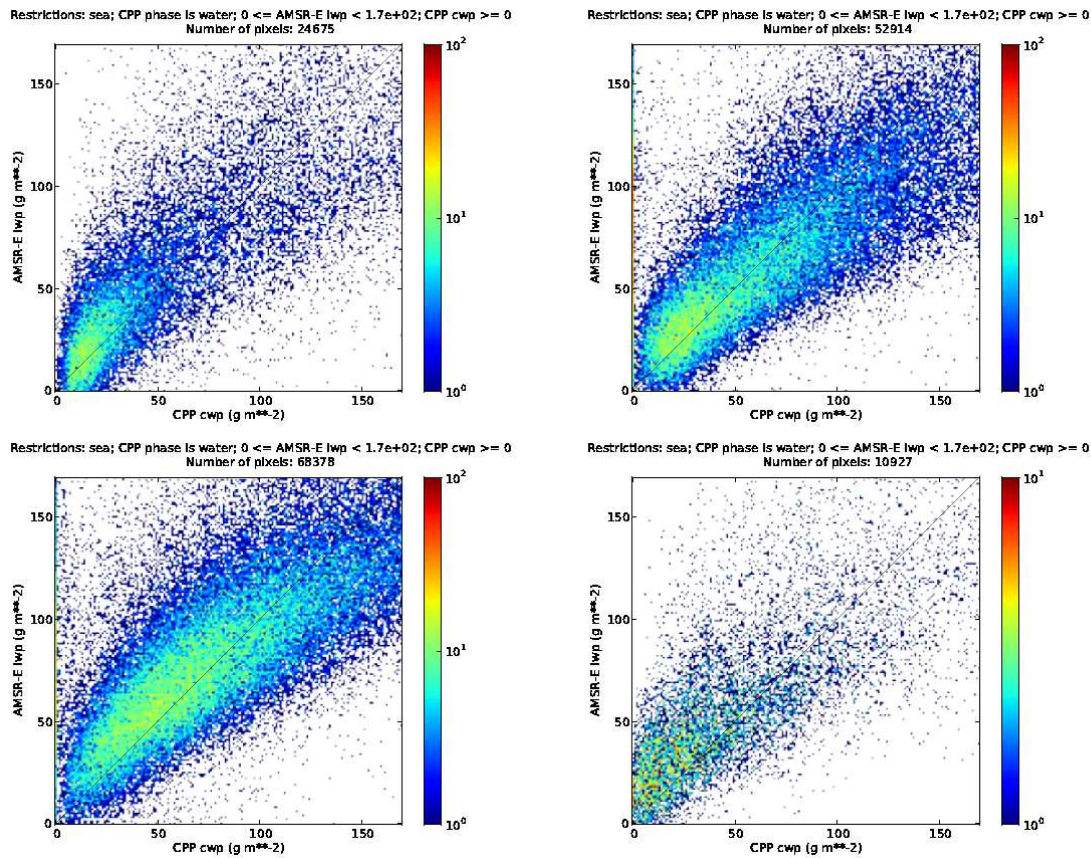


Figure 18: Scattering-density plots split by month. The colour marks the density of hits in the plotted space. Upper left: January, upper right: April, lower left: July and lower right October. The CPP values here are displayed only up to a value of 170 g/m². An example for the whole dataset in full range is shown in.

The January part of the scattering density plots, and to some extent even October, (upper left and lower right of Figure 18) show a general underestimation of liquid water path when it is low (AMSR-E LWC < 50 g/m²). This is also depicted by a negative bias for October (mean difference in Figure 19, lower right). For all months under investigation, the slope of the scatterplot deviates from the optimal 1:1 diagonal, with underestimation for low values and an overestimation in the high value range. The differences in statistics (especially the bias) are explained by the skewness of the distribution, which varies from month to month and with it the balance point between lower and higher values.

The deviation histograms show (except for July) a pronounced tail, to overestimations as well as to underestimations. These extreme values control the most part of the RMS error.

July and October show a relatively low bias which may be because of compensating effects from overestimated high and underestimated low LWP values. On the other hand, only the April case from the other tested sub-samples exceeds the threshold accuracy given by the PRD.

The RMS error is for all four months under the threshold accuracy, and for April, July and October under the given target accuracy. The bias is for January and April under the given threshold accuracy, for July under the target accuracy and for October under the optimal accuracy.

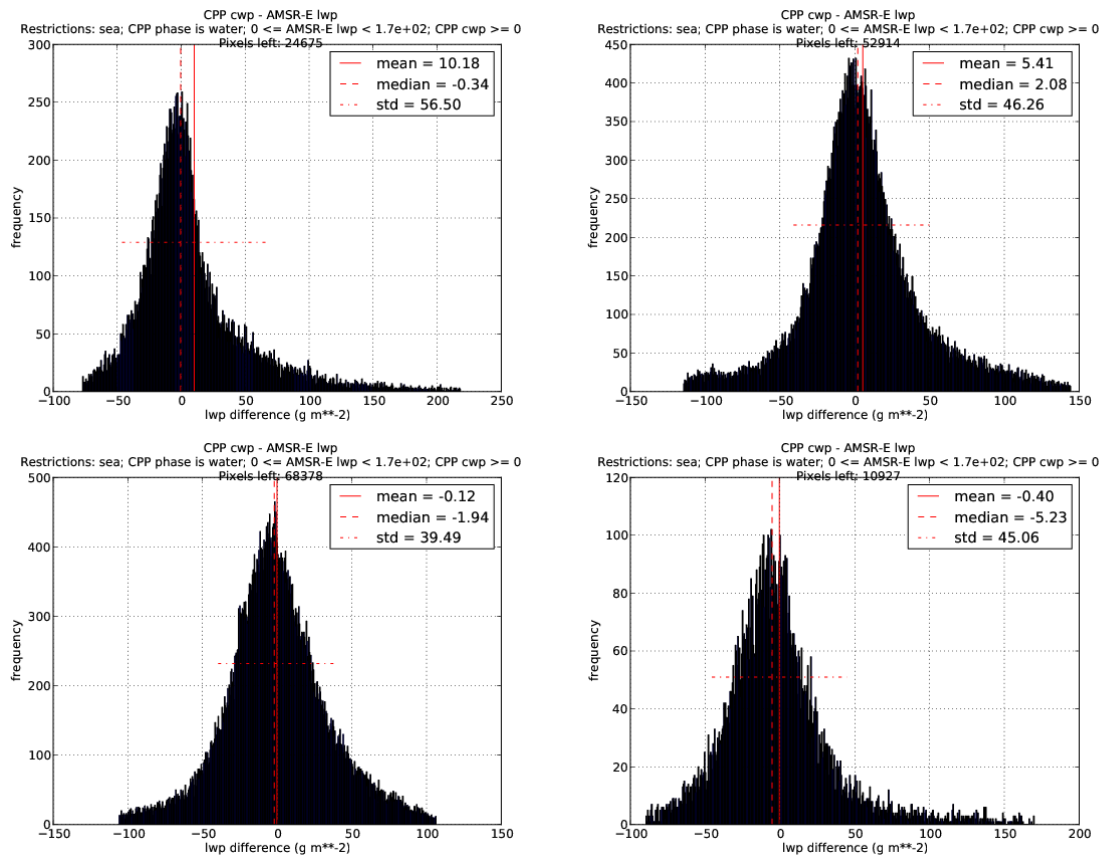


Figure 19: Histograms of deviation CPP – AMSR-E. In this sense ‘mean’ is equal to the error description Bias and ‘std’ is equal to the BC RMS error. To keep focus on important features, this and the following deviation histograms show data between the 1 and 99 percentile only. Upper left: January, upper right: April, lower left: July and lower right October.

Table 23: Achieved accuracy (values for version 2012 in brackets) and requirements for LWP product.

	RMS [g/m ²]	Bias [g/m ²]
Achieved accuracy, day	45.39 (47.0)	3.35 (6.3)
Threshold accuracy	≤ 100.	≤ 20.
Target accuracy	≤ 50.	≤ 10.
Optimal accuracy	≤ 20.	≤ 5.

4.4.2.2 Study of performance under different illumination conditions

The version 2014 of CPP has an extended valid range for solar zenith angles. In previous versions, calculations of the LWP product were possible for solar zenith angles up to 72°. Version 2014 allows for production up to 84°. So a simple test of performance under different illumination conditions has been realised. This study was made with a preliminary version of 2014, but the conclusions should be valid for version 2014 as well.

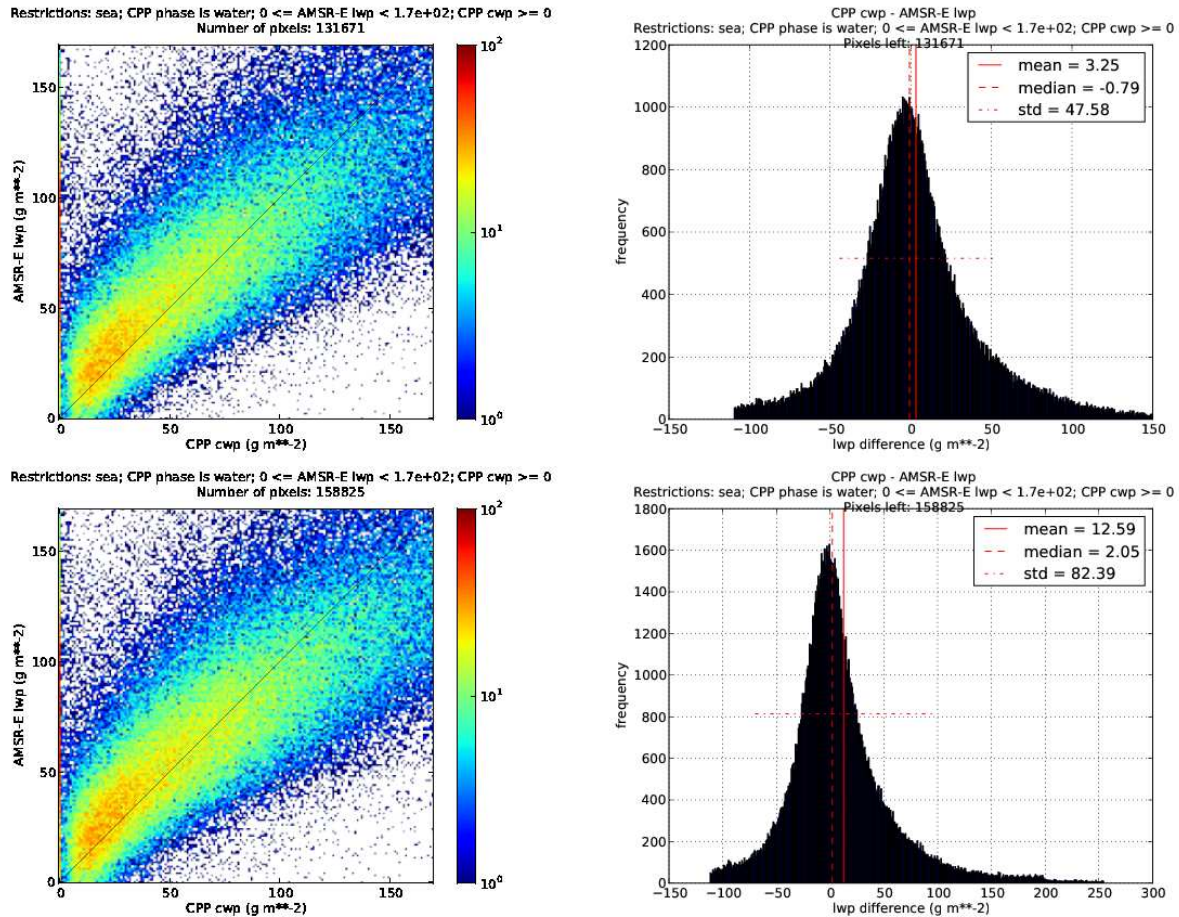


Figure 20: Scattering density (left column) and histogram deviations (right column) for only daytime pixels (solar zenith angle below 72°, upper row) and entire dataset (solar zenith angle up to 84°, lower row). Note the different scaling for histograms in right column.

In Figure 20 it is shown how results of the LWP product look like under different light conditions. The overall pattern of distribution (left side) looks almost identical. However, the coil is sharper or less (lateral) elongated if only daytime pixels (in the definition of version 2012, which is a restriction to solar zenith angles below 72°) are taken into account. This is also reflected in the histograms (right side). Here both, bias as well as standard deviation increases remarkably, when the range of allowed solar zenith angles is widened to 84°. In other words, accuracy decreases from target to threshold accuracy (bias and RMS error).

We think that it is at least questionable if the loss in accuracy is justified by the gain in a number of pixels (about 17000 in this case). See detailed numbers of achieved and required accuracies in Table 24. This table illustrates also that for sun zenith angles lower than 72degree, performance with

<i>EUMETSAT Satellite Application Facility to NoWCasting & Very Short Range Forecasting</i>	Scientific and Validation Report for the Cloud Product Processors of the NWC/PPS	Code: NWC/CDOP2/PPS/SMHI/SCI/VR/Cloud Issue: 1.0 Date: 15 September 2014 File: NWC-CDOP2-PPS-SMHI-SCI-VR-Cloud_v1_0 Page: 57/67
---	--	---

respect to random errors is similar between versions 2012 and 2014, while the bias is slightly lower for the validation dataset. Scatterplots and error distributions for both versions show very similar algorithm behaviour, not discernable by visual inspection (not shown).

For version 2014, more colocations were found with the same validation dataset. It is worth to pointing out that a large part of these additional LWP retrievals will stem from more challenging environmental conditions as sunglint areas, which were excluded in version 2012.

Table 24: Achieved accuracy (values for version 2012 in brackets) and requirements for LWP product in different illumination.

	RMS [g/m²]	Bias [g/m²]
Achieved accuracy, day (<72°)	47.58 (47.0)	3.35 (6.3)
Achieved accuracy, whole range (<84°)	82.39	12.59
Threshold accuracy	≤ 100.	≤ 20.
Target accuracy	≤ 50.	≤ 10.
Optimal accuracy	≤ 20.	≤ 5.

For PPS v2014 the maximum sun zenith angle for LWP retrieval is configurable (maximum 84 °). Based on the results of Table 24, the recommended limit is 72°, to achieve the desired quality of the product.

4.4.2.3 Global validation of LWP

In order to expand the validation to global scale, 99 PPS GAC scenes from year 2006 to 2009 were matched to AMSR-E observations. The same restrictions as used in section 4.4.2.1 were applied here with the exception that focus was put on day-like illumination condition (i.e. the minimum solar zenith angle was set to 72°) and – after a visual inspection and careful consideration – the upper limit of CPP LWP was set to 3000 g/m².

Figure 21 gives an impression of the global distribution of data. It also shows that the given limit of a maximum LWP for the AMSR-E product turns into a quasi-spatial filter since it sorts out tropical measures with pronounced high liquid water contents. Unfortunately this is the only method to remove all rain-contaminated pixels. PPS derived liquid water paths of 170 g/m² or higher can not be validated but compared to the MODIS product. This is discussed in section 4.4.2.4 below.

Collocated PPS - AMSR-E lwp

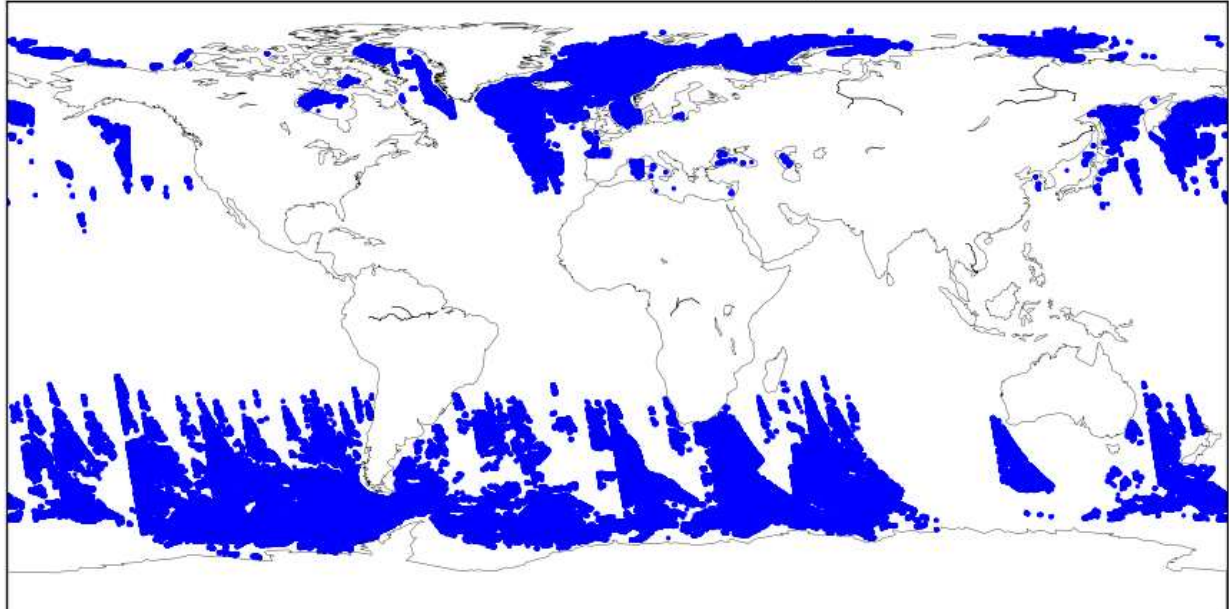


Figure 21: Data-coverage of global GAC-AMSR matches. A total of 1108330 collocated data points met the requirements for this study.

Deviations on pixel base are visualized in the scattering density plot, Figure 22 (note, that both axes are logarithmic). The orientation of the data-lobe deviates from the 1:1 line. The CPP LWP product overestimates high values and underestimates low values. This pattern has also been observed in the local dataset of the EARS region (cf. Figure 20).

Figure 23 shows the distribution of differences between PPS and AMSR-E LWP product. Lower and upper limits of the function (negative and positive end) are marked by the upper limits of both data-sets (170 g/m^2 for AMSR-E and 3000 g/m^2 for PPS). The numerical values of the plotted bias and RMS error are also given in Table 25. There it is shown that the RMS error of 96.5 g/m^2 meets the requested threshold accuracy of 100 g/m^2 while the bias, calculated with 29.5 g/m^2 misses the threshold of 20 g/m^2 . Here it could be helpful to discuss, whether the applied limits, e.g. the maximum LWP of 3000 g/m^2 or the maximum solar zenith angle of 72° are suitable. Kato and Marshak (2009) showed that the retrieval quality for cloud optical thickness, which is an important product on the way to the liquid water path, depends strongly on viewing and illumination geometry.

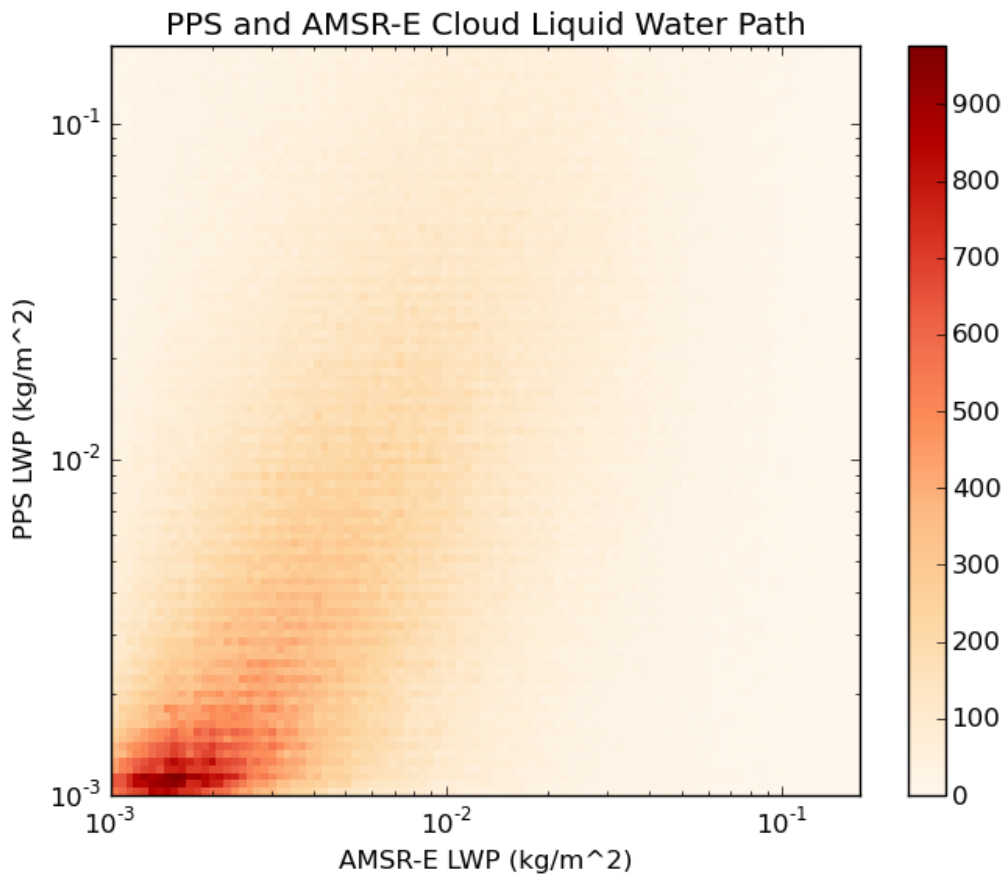


Figure 22: Scattering density diagram of AMSR-E LWP product and CPP LWP product.

Table 25: Required and achieved accuracies for the global validation activities.

	RMS [g/m²]	Bias [g/m²]
Achieved accuracy	96.5	29.5
Threshold accuracy	≤ 100.	≤ 20.
Target accuracy	≤ 50.	≤ 10.
Optimal accuracy	≤ 20.	≤ 5.

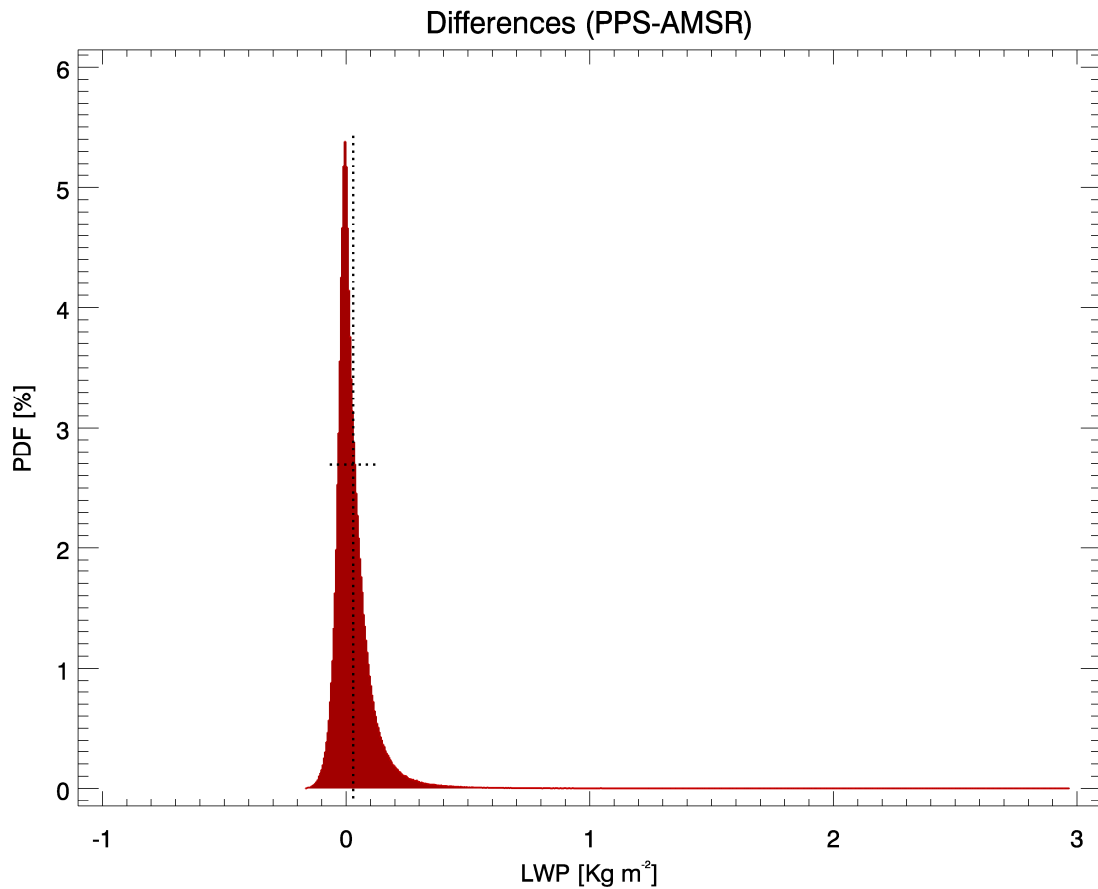


Figure 23: Probability density function of differences between PPS LWP product and AMSR-E LWP product. The vertical dotted line marks the bias (29.5 g/m²) while the horizontal dotted line illustrates the RMS deviations (96.5 g/m²).

4.4.2.4 LWP comparison land/sea

None of our activities towards a reasonable validation of the CPP liquid water path product over land was successful so far. Finally we came to the conclusion, that a comparison with the MODIS liquid water path product would enable at least a cautious assessment of the performance over land.

Based on the PPS GAC scenes used for the inter-comparison with the AMSR-E LWP product, MODIS-AQUA pixel were also collocated with GAC pixel to allow for an inter-comparison of both LWP products. The MODIS LWP product is, in contrast to the AMSR-E product, also valid over land. The disadvantage is that the MODIS algorithm is based on a similar retrieval techniques (even though, the MODIS features more channels and different channel characteristic) and can not count as an independent or, even more important, superior product to allow proper validation. A comparison of the results for sea-only and land-only may provide anyhow valuable information about systematic differences or difficulties.

Collocated PPS-MODIS lwp, all surface-types

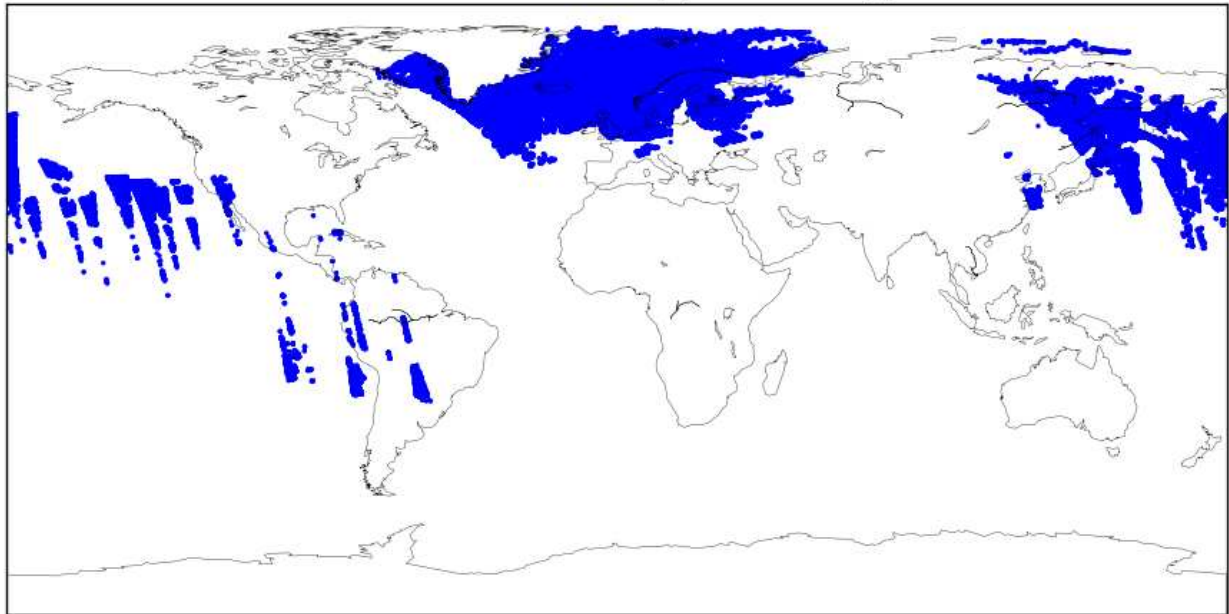


Figure 24: Global distribution of PPS - MODIS matches for the selected GAC scenes. The total number of collocated pixel is 838851.

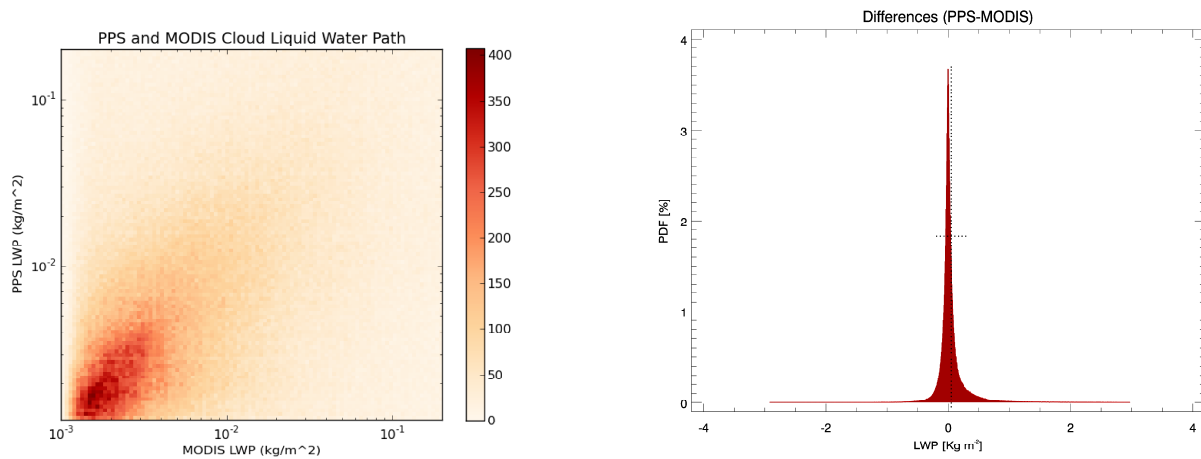


Figure 25: Scattering density (left) and probability density of deviations (right) for PPS – MODIS matches. Additionally, the right image provides information about the bias (vertical dotted line, here 49.0 g/m²) and the RMS deviation (horizontal dotted line, here 246.2 g/m²).

The distribution of all available PPS – MODIS collocations (sea and land) is shown in Figure 24. It is obvious that the emphasis lies on the northern hemisphere.

Corresponding scattering density and probability of differences are displayed in Figure 25. No substantial pattern of deviation from the 1:1 in the scattering density plot line is visible by eye. However, the statistical values of bias (49.0 g/m²) and RMS deviation (246.2 g/m²) marked in the

probability density plot are considerably higher compared to results with the AMSR-E product as a reference.

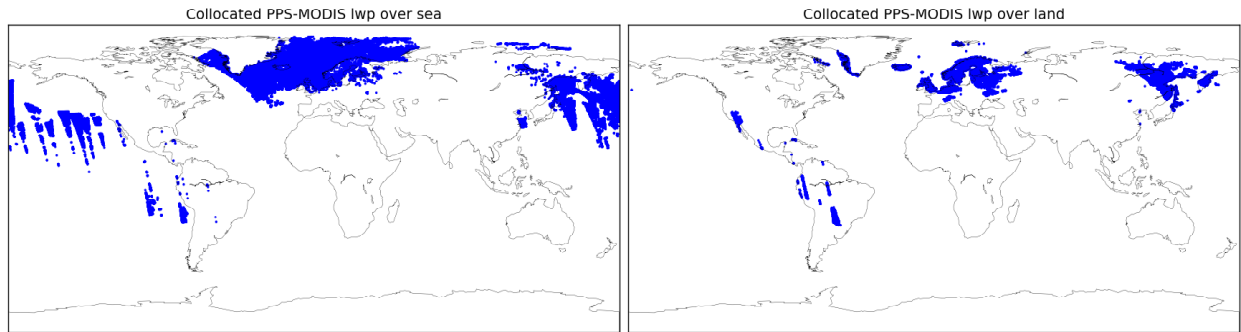


Figure 26: Global distribution of PPS – MODIS matches over sea (left) and over land (right). In total, 735752 of the selected pixel are over sea and 103099 are over land.

To achieve better insight into the influence of the characteristic of the surface on LWP retrievals, the dataset was split into sea and land pixels. Figure 26 gives an overview of their global distributions. Note that the number of sea pixels (735752) is bigger than that of land pixels (103099). Scattering density and probability density of differences are shown in Figure 27 and Figure 28.

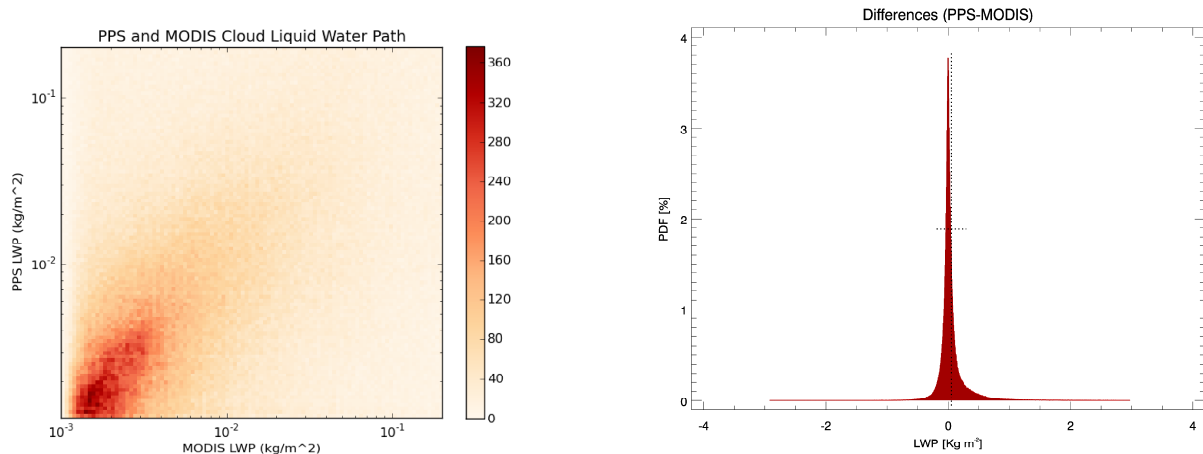


Figure 27: Same as Figure 25 but only sea pixels are considered. The bias here is 52.6 g/m² and the RMS deviation is 242.0 g/m².

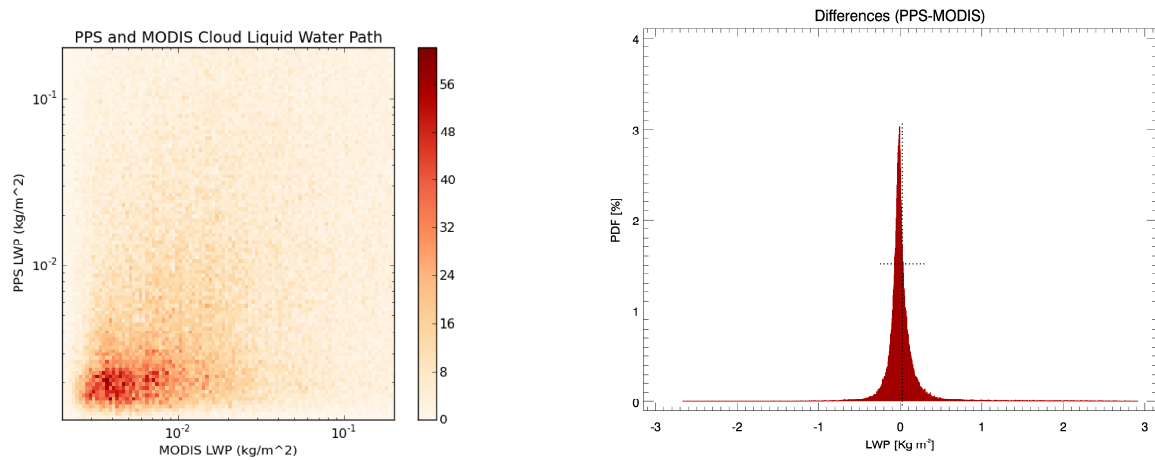


Figure 28: Same as Figure 25 but only for pixels over land. Here the bias is 23.6 g/m^2 and the RMS deviation is given with 273.2 g/m^2 .

From visual inspection, the scatterplot of the land pixel looks worse (i.e more random distributed and less concentrated around the 1:1 line). Also the width of the PDF for land pixels seems to be more distinct than that of sea pixels. The numbers (at least the RMS, compare Table 26) support this impression. However, differences are small and may even be related to noise.

If the results over sea are considered acceptable, then, just looking at the numbers, the results over land with slightly worse RMS deviations and slightly better biases should also considered acceptable.

Table 26: Overview: Statistical values for the intercomparison of MODIS and PPS LWP product.

	RMS [g/m²]	Bias [g/m²]	N
All pixels	246.2	49.0	838851
Sea pixels	242.0	52.6	735752
Land pixels	273.2	23.6	103099

4.5 PRECIPITATING CLOUDS

The product Precipitating Clouds has not undergone any scientific changes for PPS v2014, thus there were no need to validate it. Latest validation of the Precipitating Clouds product is found in [RD.3b].

<i>EUMETSAT Satellite Application Facility to NoWCasting & Very Short Range Forecasting</i>	Scientific and Validation Report for the Cloud Product Processors of the NWC/PPS	Code: NWC/CDOP2/PPS/SMHI/SCI/VR/Cloud Issue: 1.0 Date: 15 September 2014 File: NWC-CDOP2-PPS-SMHI-SCI-VR-Cloud_v1_0 Page: 64/67
---	--	---

5 SUMMARY AND CONCLUSIONS

In this report we validate the 2014 version of PPS for AVHRR and VIIRS data. The validation is made for the PGEs (01, 02, 03, 05-CPP phase and 05-CPP LWP). For PGE01 validation is performed against a comprehensive dataset of global Synop reports (kindly provided by DWD). Two collocation datasets have been used, one with direct readout S-NPP, NOAA-18 and 19 received at SMHI, and another using a global dataset of 99 AVHRR GAC orbits from 2006 to 2009. For PGEs 01-03 we furthermore use a collocation dataset of AVHRR and VIIRS matched with a set of CALIPSO lidar products: Both matchups from 17 months of CALIPSO and Suomi-NPP/NOAA18-19 data locally received at SMHI in Norrköping as well as the dataset of 99 AVHRR GAC orbits for 2006-2009 have been used for PGE 01-03.

For the PGE05 validation we use 4 months of EARS AVHRR data in 2010, and validate with CALIPSO cloud phase and AMSR-E LWP data. Additionally, we use matches of the 99 AVHRR GAC data with AMSR-E LWP observations to validate the CPP LWP product on a global scale. Furthermore, we try to close the gap which opens due to a lack of reference LWP observations over land with sufficient data coverage by an inter-comparison of these global GAC data with the MODIS LWP product.

We find that quite a number of target accuracies are reached, and that most scores are within threshold accuracy. We also show many examples of how the PGE01 and PGE03 have improved compared to PPS v2012/v2010.

The cloud mask is meeting the target accuracy globally under all illumination conditions according to the Synop validation, and over the European domain (including the Arctic) the target accuracy is being met in daytime. The AVHRR GAC based dataset filtered over Europe actually show that the cloud mask is performing according to the target accuracy, while the more comprehensive Synop based dataset (that also include more Arctic stations) only meet the target accuracy in daytime, whereas at night and twilight the threshold accuracy is passed with a large margin.

Using CALIPSO as the reference truth for the cloud mask over Europe (Norrköping direct reception area) the threshold accuracy (for POD-cloudy and FAR-cloudy) is passed for all cases (after filtering the CALIPSO data by optical thickness). However, without any filtering for cloud optical thickness (allowing for even the thinnest clouds detected by CALIPSO which are undetectable by AVHRR/VIIRS) the POD-cloudy is below the threshold accuracy in night and twilight. For the FAR-cloudy the target accuracy is reached/passed for all cases (both filtered and unfiltered), but the FAR-clear is high and around and even above 30%. But again it is important to emphasize that also those scores have been significantly improved against previous PPS versions. Then it should be noted that the original score requirements were defined for validations against Synop reports.

For the cloud type and the separation in low, medium level and high clouds, the low and high clouds match either target or threshold accuracy for both POD and FAR in all cases, but the medium level clouds does not quite meet the threshold accuracies.

The CTTH product have been considerably improved over previous versions, in particular giving many more valid results for semi-transparent clouds while at the same time retaining or improving the validation scores. However, the threshold accuracy is still not met for high clouds, being it opaque or semi-transparent. One exception is the bc-RMS score for high semi-transparent clouds, where for the first time the threshold accuracy is just passed. Otherwise both the bias and bc-RMS is still quite far from the threshold accuracy for high clouds.

<i>EUMETSAT Satellite Application Facility to NoWCASTing & Very Short Range Forecasting</i>	Scientific and Validation Report for the Cloud Product Processors of the NWC/PPS	Code: NWC/CDOP2/PPS/SMHI/SCI/VR/Cloud Issue: 1.0 Date: 15 September 2014 File: NWC-CDOP2-PPS-SMHI-SCI-VR-Cloud_v1_0 Page: 65/67
---	--	---

For low and medium level clouds in general the target accuracy is reached, and even the optimal accuracy is reached for medium level cloud assignment in the semi-transparent retrieval.

For the CPP LWP within the EARS domain all thresholds are met. The global GAC data miss the bias but reach the RMS requirement. CPP liquid water path product (LWP) is not validated over land because microwave observations over land are subject to a different physical principle compared to liquid water path (LWP) deductions over ocean. Other sources provide LWP products even over land but they lack superior accuracy, which is needed for a proper validation or reasonable temporal/spatial coverage for a thorough validation. However, a comparison of global GAC LWP data with the MODIS LWP product shows that RMS deviations and bias for over land and over sea are in the same order of magnitude. Even if there is no actual validation of the liquid water path over land, there is however a case study with the focus on clouds in coast regions [RD.3.], together with the recent inter-comparison with product from other sensors (4.4.2.4), do point in the right direction. Future validation activities will set priorities on these inter-comparison strategies.

For CPP cloud phase, both data sets, the EARS domain as well as the global GAC data, meet all required thresholds. Only few of the sub-samples of the cloud phase product miss them. This may be due to biased weighting as a result of sampling only specific situations. Compared with version 2012, the current results show a more balanced behaviour and are applicable to a wider range of solar zenith angles. The *lwp* product bias shows indications of compensating effects. This is not critical as long as no extreme (low or high) LWP values dominate the dataset. In general the results of sub sample variations for the official CPP products show a more stable behaviour than that of version 2012. For low solar zenith angles (daytime) the success measures have improved remarkably. Processing of pixels with lower sun elevation was not even possible in version 2012.

<i>EUMETSAT Satellite Application Facility to NoWCASTing & Very Short Range Forecasting</i>	Scientific and Validation Report for the Cloud Product Processors of the NWC/PPS	Code: NWC/CDOP2/PPS/SMHI/SCI/VR/Cloud Issue: 1.0 Date: 15 September 2014 File: NWC-CDOP2-PPS-SMHI-SCI-VR-Cloud_v1_0 Page: 66/67
---	--	---

6 REFERENCES

- CMSAF Validation Report, 2009: Climate Monitoring SAF Annual Validation Report. Reference Number: SAF/CM/DWD/VAL/OR5.
- Greenwald, T.J., 2009: A 2 year comparison of AMSR-E and MODIS cloud liquid water path observations, *Geophys. Res. Lett.*, 36, L20805, doi:10.1029/2009GL040394.
- Karlsson, K.-G. and A. Dybbroe, 2010: Evaluation of Arctic cloud products from the EUMETSAT Climate Monitoring Satellite Application Facility based on CALIPSO-CALIOP observations, *Atmos. Chem. Phys.*, 10, 1789-1807, doi:10.5194/acp-10-1789-2010, 2010.
- Karlsson, K.-G. and E. Johansson, 2013: On the optimal method for evaluating cloud products from passive satellite imagery using CALIPSO-CALIOP data: example investigating the CM SAF CLARA-A1 dataset, *Atmos. Meas. Tech. Discuss.*, 6, 1093-1141.
- Kato, S. and A. Marshak, 2009: Solar zenith and viewing geometry-dependent errors in satellite retrieved cloud optical thickness: Marine stratocumulus case, *J. Geophys. Res.*, 114, doi: 10.1029/2008JD010579.
- Minnis, P., C. R. Yost, S. Sun-Mack, and Y. Chen (2008), Estimating the top altitude of optically thick ice clouds from thermal infrared satellite observations using CALIPSO data, *Geophys. Res. Lett.*, 35, L12801, doi:10.1029/2008GL033947.

<i>EUMETSAT Satellite Application Facility to NoWCasting & Very Short Range Forecasting</i>	Scientific and Validation Report for the Cloud Product Processors of the NWC/PPS	Code: NWC/CDOP2/PPS/SMHI/SCI/VR/Cloud Issue: 1.0 Date: 15 September 2014 File: NWC-CDOP2-PPS-SMHI-SCI-VR-Cloud_v1_0 Page: 67/67
---	--	---

ANNEX A. List of TBC, TBD, Open Points and Comments

TBD/TBC	Section	Resp.	Comment